

UNIVERSITAT POLITÈCNICA DE CATALUNYA

MASTER THESIS

Controlling a Quadrotor with a Robotic Arm using a Nonlinear Model Predictive Control

Author:

Sebastián Chávez-Ferrer Marcos

Supervisors:

Dr. Carlos Ocampo Martínez

Institut de Robòtica i Informàtica Industrial (CSIC-UPC)

January 2015

Acknowledgements

I would like to express my gratitude to the Master coordinator, Cecilio Angulo, who helped me to solve all my administrative problems and also who showed me the benefits of the master.

Also, I would like to thank my supervisor Carlos Ocampo, who guided me through the good and bad moments of the thesis. Without his help it would have been impossible to finish it.

On the other hand, I would like to express my appreciation to all the people from the Institut de Robòtica i Informàtica Industrial (IRI) where I was very well welcomed.

I would like to thank all the people who suffered and enjoyed this Master with me, my class colleagues from the MAiR and my friends from ETSEIB.

Additionally, I would like to thank Victor, Neus and Paula to help me finish this project.

Finally I would like to express my biggest acknowledgements to my parents, who supported me and encouraged me until the end of my studies.

Abstract

This thesis presents a method to control a quadrotor equipped with a robotic arm. The arm has been developed in the Institut de Robòtica i Informàtica Industrial (CSIC-UPC).

During the project, an algorithm has been made as a first approximation to control a quadrotor which is working with the robotic arm.

In order to compensate the perturbations of the arm's dynamic, a nonlinear model predictive control algorithm has been chosen among other possible techniques. (PID, Model Predictive Control or LQR).

PID and model predictive control have been discarded because it is not possible to control the nonlinearities of the system studied with an appropriate accuracy.

Finally, five scenarios have been simulated and tested to verify the performances and robustness of the designed method. First of all, a takeoff maneuver, where the quadrotor reaches to a specific altitude. Also, a hover mode where the system has to compensate the dynamics of the arm while it is static or it is in movement. Finally, the quadrotor has to move to a specific point in space while the arm is static or in movement.

The goal of design a controller is to reject the perturbation due the arm and stabilize the system.

This thesis presents the results obtained after testing the controller designed with the scenarios created.

Contents

Acknowledgements	iii
Abstract	v
List of Figures	ix
List of Tables	xi
Nomenclature	xiii
1 Introduction	1
1.1 Motivation	1
1.2 Objectives	2
1.3 Scope of Research	2
1.4 Outline of the Thesis	3
2 Background	5
2.1 Unmanned Aerial Vehicles	6
2.2 Robotic arms	7
2.3 Control Algorithms	8
2.4 State of the art	12
3 Case Study Description and Control Problem	15
3.1 Quadrotor Description	15
3.1.1 Dynamic Equations of a X-Type Quadrotor	15
3.1.2 Dynamic Equations to Simulate the Real Plant	22
3.1.3 Physical and Geometrical Parameters of the Quadrotor Model	23
3.2 Robotic Arm Description	24
3.2.1 Dynamic Equations of a Robotic Arm	24
3.2.2 Dynamic equations to Simulate the Real Robotic Arm	28
3.2.3 Physical and Geometrical Parameters of the Arm Model	29
3.3 NMPC Problem Statement	31
3.3.1 Dynamic model	32
3.3.2 Objective function	34
3.3.3 Constraints	36
3.3.4 Optimization Problem	39
4 Simulation Results	41
4.1 Take off	45

4.2	Quadrotor in a fixed position	50
4.2.1	Robotic Arm in a fixed position	51
4.2.2	Robotic Arm in movement	53
4.3	Quadrotor in movement	54
4.3.1	Robotic Arm in a fixed position	55
4.3.2	Robotic Arm in movement	57
5	Conclusions and Future Work	61
5.1	Conclusions	61
5.2	Future Work	62
	Bibliography	65

List of Figures

2.1	Top-Left: X-Type. Top-Right: V-Type. Bottom: Stingray-Type	7
2.2	Robotic arm designed by CSIC-UPC	8
2.3	Scheme of MPC algorithm	10
2.4	NMPC scheme	11
2.5	Examples of UAV	13
3.1	Blade system reference	16
3.2	Forward-Backward movement	18
3.3	Left-Right movement	19
3.4	Up-Down movement	19
3.5	Rotate around E_a^3	19
3.6	Parameters of a blade	20
3.7	Denavit hartenberg parameters	26
3.8	Matlab model of the robotic arm designed by CSIC-UPC.	30
4.1	Arm robotic in the safe position	42
4.2	Dynamic Reaction in the base of the arm when remains in a fixed position	43
4.3	Reference and Angle of each joint	44
4.4	Dynamic Reaction in the base of the arm due its motion	45
4.5	Cost function during the Take Off	47
4.6	Control signal for a Take Off	48
4.7	State variables for the Take off	49
4.8	State variables for a quadrotor in a fixed position and an arm in a fixed position	51
4.9	Cost function for a quadrotor in a fixed position and an arm in a fixed position	52
4.10	State variables for a quadrotor in a fixed position and an arm in movement	53
4.11	Cost function for a quadrotor in a fixed position and an arm in movement	54
4.12	Cost function for a quadrotor in movement and an arm in a fixed position	55
4.13	State variables for a quadrotor in movement and an arm in a fixed position	57
4.14	Cost function for a quadrotor in movement and an arm in movement . . .	58
4.15	State variables for a quadrotor in movement and an arm in movement . .	59

List of Tables

3.1	DH parameters of the robotic arm	31
4.1	Initial Conditions for Take Off	46
4.2	Summary of Take Off	49
4.3	Initial Conditions for Static Control	50
4.4	Summary of the control for a quadrotor in a fixed position and an arm in a fixed position	52
4.5	Summary of the control for a quadrotor in a fixed position and an arm in movement	54
4.6	Initial Conditions for the trajectory of the Quadrotor	55
4.7	Summary of the control for a quadrotor in movement and an arm in a fixed position	56
4.8	Summary of the control for a quadrotor in movement and an arm in movement	59

Nomenclature

m	Mass of the Rotor	kg
I	Rotational inertia	kg m^2
ρ	Density of the air	kg / m^{-3}
g	Acceleration due the gravity	m s^{-2}
r_r	Rotor radius	m
A_r	Rotor disc area	m^2
ω_r	Angular velocity of the rotor r	rad s^{-1}
$sk(\Omega)$	Skew-Symmetric matrix	Non-dimensional
R	Rotation matrix	Non-dimensional
D_r	Rotor displacement from the flyer center of mass	m
CoG	Center of gravity	m
T_r	Thrust of the rotor r	N
Q_r	Thrust of the rotor r	N m
M_r	Momentum due the displacement of the thrust	N m
C_Q	Torque coefficient	Non-dimensional
C_Q	Thrust coefficient	Non-dimensional
$a1s_r$	First-harmonic solution of the longitudinal flapping coefficient	rad
$b1s_r$	First-harmonic solution of the lateral flapping coefficient	rad
σ	Rotor Solidity	Non-dimensional
a	Blade lift slope gradient	Non-dimensional
c	Blade chord	m
I_b	Rotor blade rotational inertia about the flapping hinge	kg m^2

Chapter 1

Introduction

1.1 Motivation

In the last years there has been an increasing importance of quadrotors in society and also of the tasks that they can do. There is a need for extending the capabilities of a quadrotor to satisfy the increasing demand of new services from the companies.

The motivation of this project is to provide a Nonlinear Model Predictive Control (NMPC) for a quadrotor's robotic arm attached to its body. Most of the literature explains methods about how to control an Unmanned Aerial Vehicle applying a model predictive control to a linearized model, like in [Bouffard \[2012\]](#). Other kind of papers are focused on finding an appropriate mathematical model that explains most of the dynamic effects that occur during the maneuvers as it is well explained in [Pounds et al. \[2006\]](#). But there are also few papers like [Bangura and Mahony \[2012\]](#) that try to control the quadrotor by using a nonlinear model predictive control algorithm.

The quadrotor in which this research is based has been described in [Sanramaria and Andrade \[2014\]](#) and it is used by Institut de Robòtica i Informàtica Industrial (CSIC-UPC), on its research in the Aerial Robotics Cooperative Assembly System ARCAS European project. This European project has the goal of design and develop cooperating flying robots for assembly operations. This quadrotor will have to be able to cooperate with other robots in order to accomplish different goals like surveillance, assembly structures or track and detect objects.

With this thesis a new approach to control a quadrotor with a robotic arm is going to be presented.

1.2 Objectives

The main goal of this project is to use the NMPC method to control a quadrotor like in the existing literature. The new feature added is that the quadrotor has a robotic arm attached to its body and the NMPC has to compensate the perturbations generated by the motion of this arm. The thesis presented here has the aim of developing a first approach of a controller able to manage these perturbations. More specific objectives have been proposed as follows:

1. To design an algorithm to study the viability of the control.
2. To discretize and implement to Matlab environment the dynamic equations of the quadrotor and the robotic arm.
3. To couple the dynamic effects of the quadrotor and the arm.
4. To build a real parametrized model of a quadrotor and a robotic arm.
5. To design a NMPC to control the dynamics and carry the system to specific operational points.
6. To analyse the stability of the quadrotor while it is holding a position and the arm is in a fixed pose or in movement.
7. To analyse the stability of the quadrotor while it is in movement and the arm is in a fixed pose or in movement.

1.3 Scope of Research

Some decisions have been taken by an heuristic method since were out of the scope of this research.

The sampling time and the control horizon have been chosen in order to properly run the simulations and verify the tests but in any case they have been optimized to run the NMPC algorithm at the fastest velocity.

The aim of this project is to design a NMPC for a simulation environment, so the code is not optimized to use it in real time. Moreover, the identification of the models is out of the study proposed. During this thesis, parameters chosen to design the model of the quadrotor and the arm have been mixed from different researches. However, all the values selected have been verified to ensure that they were real and possible values. Finally, the trajectory made by the arm is not controlled by the NMPC. Multiples PD have been designed to control each joint. Performance and stability of its trajectory are not taken into account during this study.

1.4 Outline of the Thesis

This study is organised as follows:

Chapter 2 - Background: The background contains all the theoretical information that is necessary to understand implementation and results. At the beginning a description of the state of the art has been presented. Below there is a detailed explanation about the UAV, the robotic arm and the control algorithm chosen for this study.

Chapter 3 - Implementation: In chapter 3 a description of the implementation has been presented. There is a detailed description of the equations that define the dynamics of the quadrotor and the robotic arm. There is also a explanation about the parameters that define the model of each device. Finally the NMPC designed is presented with all its features.

Chapter 4 - Results: In chapter 4 there are the results of the five scenarios that have been tested. Each section has a brief description about the initial conditions and a summary with the results obtained. Additionally in this chapter we have a description of the perturbations given by the arm.

Chapter 5 - Conclusions and Future Work: Conclusions derived from these results are presented in this chapter. It is commented the goals achieved and possible



failures that happened. It is detailed possible improvements and fields with a interesting line of research.

Chapter 2

Background

In this chapter the three main elements used during this project have been described:

The first element is an UAV, more specifically a quadrotor. In these times, it is the most popular vehicle in the commercial field and so the most studied system, apart from being the cheapest model that can be found. This reasons are the ones why most of researcher laboratories are focusing their studies on this system.

The second element is a robotic arm. This mechanism increases the versatility of the quadrotor. At present there are lots of types of robotics arms. Considering that a quadrotor has a small payload, the arm has to be light but strong enough to carry the maximum weight that is possible. So, in that case, the robotic arm designed in the CSIC-UPC, described in [Sanramaria and Andrade \[2014\]](#), has been chosen to test the methods explained in this thesis.

The third element is the control algorithm. A nonlinear model predictive control has been selected to control the whole system. The main reason is because most of the problems that have been had to face could be represented as an optimization problem. This implies that it is possible to solve the problem subject to certain restrictions. It is also possible, because the dynamic systems of the quadrotor and the arm are well known, to use it as a model in the controller. On the other hand, due to nonlinearities, is important to use a robust algorithm to absorb all non controlled changes.

The last section is the state of art of each of the elements described above.

2.1 Unmanned Aerial Vehicles

UAV is an acronym for Unmanned Aerial Vehicle, which is an aircraft with no pilot on board. Usually, UAVs are controlled remotely and can fly autonomously based on either pre-programmed flight or using more complex dynamics.

The UAV concept is becoming more popular each year. There are a lot of types, sizes and prices (see Figure 2.5). The purpose of this thesis is to equip an arm to a quadrotor and control its dynamics by using a nonlinear model predictive control. The robotic arm generates a perturbation that the control algorithm has to manage in order to maintain the system in a fixed position or move the quadrotor to a desired position. So an UAV with the hover capability is needed in order to hold a fixed position while an arm is working in some task.

Keeping this in mind, the most used UAV are based on a system with vertical thrust. That kind of technology consists in a generation of a vertical force to compensate the gravity component of the whole dynamic system. It is also possible, by combining the different forces generated, to obtain other forces and torques in all axis to move the robot to any position with a desired motion as it is described in [Pounds et al. \[2006\]](#).

There are several types of rotor systems in function of the task that it has to do. Depending on the autonomy, the payload or maneuverability, the number of rotors can change between models for example this eight rotor UAV described in [Romero et al. \[2009\]](#). On the other hand, other features that could change drastically the behavior of the UAV are the propellers as it explained in [Pounds \[2007\]](#) [2007].

This study is based on a model of four rotors, henceforth named quadrotor. These vehicles are used to be controlled with a electronic system able to stabilize the aircraft. These UAV can be flown indoors as well as outdoors because of the small size and agile maneuverability. However, if the quadrotor has any variable perturbation, its performance could drop until being unstable. This is the reason why it is important to design a control algorithm able to manage these perturbations.

Even in the quadrotor category, there are several types depending on the position of the rotors relative to its center of mass (X-type, V-type or Stingray-type, see Figure 2.1. During this thesis a X-Type has been chosen because their dynamic model is more

easy to manage than other kind of structures. This geometry consists in situate four rotors in a cross position with two sets of identical rotorcrafts, two of them are spinning clockwise and two counter-clockwise in order to compensate the momentum generated as it is explained in [Martinez \[2007\]](#).

A mathematical model extracted from other researches has been used to emulate its behavior in a simulation environment. The majority of papers have used the same model introduced in the nineties by [Pounds \[2007\]](#) and [Bouabdallah \[2007\]](#). In this papers, thrust and torque are modeled as a static function of the square of rotor speed. This model is based on static thrust characteristics of the rotor and holds for near hovering flights. But more complex model like [Pounds et al. \[2006\]](#) includes the effect of the rotor blade flapping and the effects of translational lift.



FIGURE 2.1: Top-Left: X-Type. Top-Right: V-Type. Bottom: Stingray-Type

This research uses a generic model of quadrotor to apply a nonlinear control to accomplish certain targets. The model chosen it is described in [Pounds et al. \[2006\]](#) and during the next chapters, a more detailed explanation about the formulation is going to be presented.

2.2 Robotic arms

There are several kind of arms and a huge number of studies about their dynamics like in [Featherstone and Orin \[2000\]](#). Implementing a robotic arm to a quadrotor would

extend the capabilities and services that an UAV could offer.

During this thesis another research group in CSIC-UPC has been working on designing a robotic arm (see Figure 2.2) able to be equipped to a quadrotor. This arm is light and enough strong to carry several tools on its end effector. Actually, this group is working on using a camera to track a tag using the quadrotor ([Sanramaria and Andrade \[2014\]](#)). In order to control both (quadrotor and arm) it is necessary to know precisely all the parameters of the robot to determine a mathematical model. Thanks to CSIC-UPC arm design, it is possible to know all this values and then use it in a simulation environment. This arm is specially designed to be equipped in a quadrotor (lightness, strength, well balanced, center of mass aligned with its base and well known model) and because of this it has been selected as the arm to be modeled and to obtain the perturbations of the system. Its dynamic has been found by using the Recursive Newton Euler algorithm as it is presented in [Khosla and Kanade \[1987\]](#).

In chapter 3 a full description of the arm and its dynamic is going to be explained.

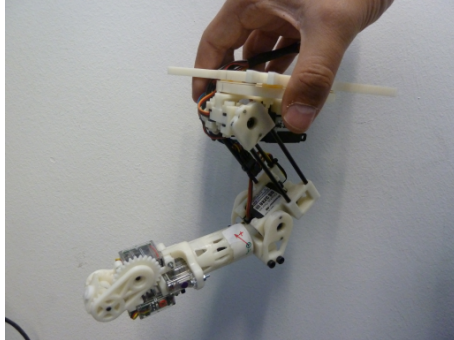


FIGURE 2.2: Robotic arm designed by CSIC-UPC

2.3 Control Algorithms

Finally, the last element necessary to control a quadrotor equipped with an arm, is its control algorithm.

At the beginning, a black box model was selected as the dynamic model of the whole system, so the first try was study the problem as generic as possible. After realizing that there are a strong coupled effects between the quadrotor and an arm, a different

strategy was chosen. Those coupled effects prevented from finding a relation between the dynamics of the quadrotor and the dynamics of the robotic arm.

As the dynamic model of a quadrotor and an arm is well known, a black box model could be discarded in order to use parametrized models. Once the model type has been chosen, the whole problem could be solved as an optimization one. Standard approaches to quadrotor control have been based on linear controller design. These methods include proportional integral derivative (PID) controllers ([Noth et al. \[2004\]](#)), linear quadratic regulator (LQR) ([Shin et al. \[2005\]](#)) or a robust H_∞ . Another method used, consists in linearize the model around a certain state of the quadrotor and then applying a predictive control model around this point like in [Bouffard \[2012\]](#) and [Bresciani](#).

A MPC has the ability to anticipate future events and can take coordinated actions by using dynamic models of the process. This algorithm is based on an iterative process which solves an optimization problem along a finite horizon. For each time t , the current plant state is sampled by using a linear model, and a minimizing of a cost function is computed for a short time horizon in the future $[t, t + N]$ (N prediction horizon). Once the problem is solved a vector of control signals is found. This vector is the trajectory of the control signals that minimize the cost function along the control horizon. From all this vector, only the control signals corresponding to the time t are applied to the real plant in the evolution of the system. Then, a new value of the state variables of the plant is obtained and the algorithm is repeated. Most of the implementations of the MPC are in discrete time where k represents the current sampled time and i the steps forward predicted as it is outlined in Figure [2.3](#).

The cost function to minimize involves all the state variables and the control signals as follows:

$$\min_u J = \sum_{i=1}^N (x_d(k+i) - x(k+i|k)) Q (x_d(k+i) - x(k+i|k))^T + \sum_{i=0}^{N_u-1} u(k+i) R u(k+i)^T$$

where $x(k+i|k)$ is the vector of the state variables, $x_d(k+i)$ is the vector reference of the state variables, the $u(k+i)$ is the control signal, Q is the weight matrix of the state variables, R is the weight matrix of the control signal, N is the prediction horizon length and N_u is the control horizon length. Also different types of cost function could be added to obtain the desired performance.

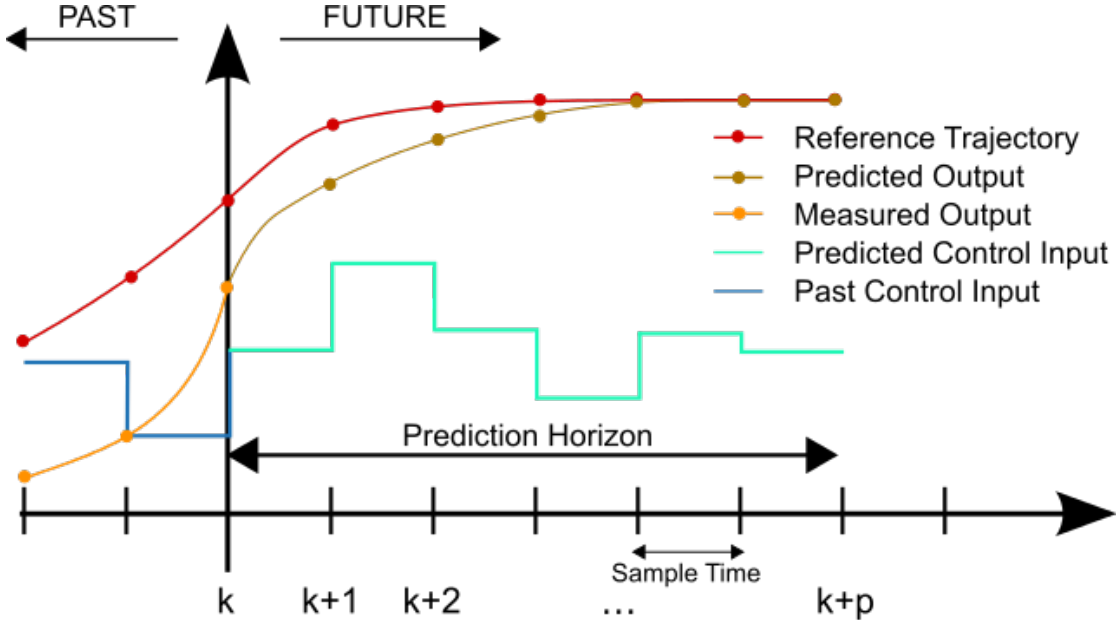


FIGURE 2.3: Scheme of MPC algorithm

The minimization of the cost function is subjected to some certain constraints defined by the designer in order to determine a state-space where the problem should be solved. To obtain the state variables in a future prediction, is necessary a mathematical model of the plant.

The main restriction of this method is that the modeled plant used on the minimization of the cost function should be linear. This method ignores most of the dynamic effects of the system and also cannot represent accurately the real behavior of the quadrotor. It's also difficult to add a new model or perturbation with this strategy.

There is a variant of this algorithm for more complex systems called Nonlinear Model Predictive Control. Adding the nonlinear part improves the response of the system at the expense of increasing the necessary computational burden.

The numerical solution of the NMPC optimal control problems is typically based on direct optimal control methods using Newton-type optimization schemes. NMPC algorithms typically take advantage of the fact that consecutive optimal control problems are similar to each other.

This allows to initialize the Newton-type solution procedure efficiently by a suitable shifted guess from the previously computed optimal solution, saving considerable amounts of computation time.

A scheme of the global workflow is presented in Figure 2.4.

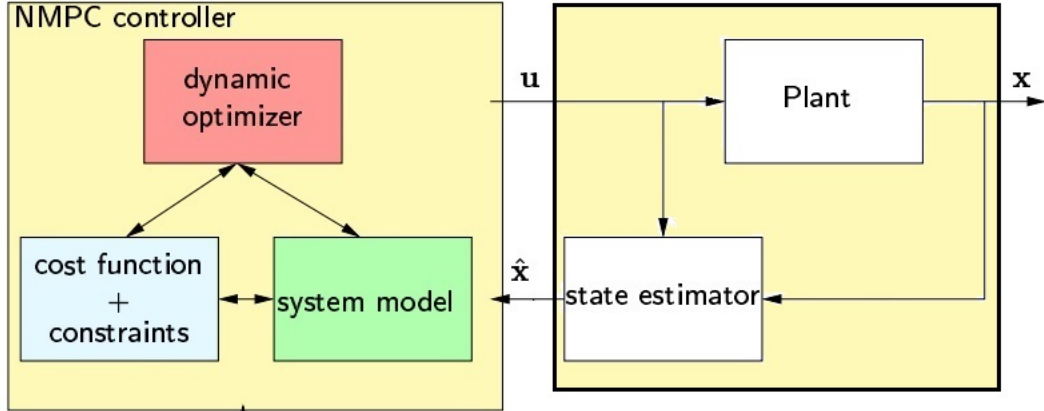


FIGURE 2.4: NMPC scheme

Plant: System to be controlled. This is the real plant which it is going to be controlled.

Usually it is difficult to obtain an appropriate model of its behaviour.

State Estimator: Make a estimation of the state variables. This method allows to do an estimation of the state of the real plant. Often the algorithm used need to apply fusion sensor to increase their accuracy. Their precision is very important to start the NMPC with the correct initial states.

Dynamic Optimizer: Solve the optimal problem. Is the element that solves the optimal problem by using the system model, the cost function and the constraints. This method has to evolve the system and find the optimal control to move the real plant to a desired state.

System Model: Mathematical model of the behavior of the plant. This model it is used to emulate the real plant and evolves the system during the optimization.

Cost Function: Function that should be minimized. This expression codifies the targets that should accomplish for each time instant. The function can weigh each objective.

Constraints: Restrictions that should be respected to solve the optimal problem. It allows to define the performance and it implements the physics restrictions of the actuators.

The Nonlinear Model Predictive Control algorithm has been chosen to control the quadrotor equipped with an arm. A more detailed explanation is presented in Section [3.3](#). On the other hand, the robotic arm has been treated as a dynamic perturbation of the quadrotor, so there is no need to control its joints. Nevertheless, it is necessary to know the exact model of the arm to calculate the dynamic reactions applied to the quadrotor due to the motion of the arm during its trajectory. The trajectory of the arm and their perturbations are calculated before applying the NMPC algorithm, so it turns out as a parameter of the system. This means that for each instant of time it is possible to know the reaction of the arm into the quadrotor. As the aim of the Thesis is to compensate this perturbation, a predictive algorithm is used to minimize the error.

The main problem of the strategy in a real case is that a good estimation of the state variables of the quadrotor it is necessary. However, this project is developed in a simulation environment, so it's possible to obtain the state variables of the plant by using a model of the system. During the next chapters, a more detailed specification of the problem will be presented.

2.4 State of the art

In the recent years, the relevance of the Unmanned Aerial Vehicles (UAV) has increased drastically. Nowadays there are a lot real examples where the UAV could be really helpful, and most of them are in the military field like in [Sydney et al. \[2013\]](#). Moreover, according to [Nonami \[2006\]](#), the UAV will be completely integrated in our society in the next few years.

Although it is possible to delegate to an UAV a lot of tasks that for a human being would take much time or even risk ([Bouabdallah et al. \[2004\]](#)), the majority of those tasks still need the human intervention to achieve their goals. Some examples could be aerial photography, television, cinema shootings ([Wai Weng \[2006\]](#)), or even uses in the research field, which sometimes needs to perform aerial experiments.

However, there exists a huge number of potential applications to be developed where the UAV could be completely autonomous. Today, most of the big companies are working on implementing new services using autonomous UAVs. Surveillance, crowd control,

mine detection or aerial delivery of payload like it is explained in [Oleg \[2009\]](#) are some of the examples.



FIGURE 2.5: Examples of UAV

In order to use autonomous UAVs it is necessary to develop new methods and algorithms to control these vehicles. The model predictive control methods used in [Raemaekers \[2007\]](#) or in [Grancharova et al. \[2012\]](#) is one clear example. However, right now almost all the external perturbations are compensated by a human. In this way, the final target is to find a method able to understand the situation, predict what is going to happen and therefore correct the behaviour of the UAV in order to accomplish the necessary performance to reach the goal.

The are several types of UAVs (see Figure 2.5) and each one reacts different in front the perturbations. At the moment, the most integrated and popular UAV in our society is the quadrotor. This mechanism was conceived in 1907 by Breguet and Richet as it is described in [Leishman \[2002\]](#). The first model was a large and heavy model that could lifted only over a small height and for short duration. After a lot of efforts the quadrotor is having the people attention and each day its relevance is increasing for the companies.

To modelling the quadrotor physics, some works like [Belkheiri et al. \[2012\]](#) and [Zhu and Huo \[2010\]](#) approximate its dynamics by a linear system, for which standard linear controllers can be designed. Other authors use nonlinear control techniques, as for example [Mellinger and V. \[2011\]](#) that used feedback linearization, [Vries and Subbarao \[2010\]](#) employing backstepping techniques, or [Benallegue et al. \[2006\]](#) developing sliding mode control. Relative to our control method, some authors like [Bangura and Mahony \[2012\]](#) have developed a nonlinear model predictive control (NMPC) to control the dynamics of a quadrotor. Other sophisticated projects have even designed a controller with a model of the wind perturbation like in [Alexis et al. \[2010\]](#).

On the other hand, the use of robotics arms in the society is widespread in several areas. Some examples can be the use of robotic arms for cooperation tasks as did [Hayati \[1986\]](#),

space as in Fukuda [1985] or even surgery as Velliste et al. [1995] did. Moreover, there are a lot of studies and works about how to control and minimize errors, like in Bicchi and Tonietti [2004], and their dynamics and behaviors are well known by studies like Herrera et al. [2012]. In this way, it is a good choice to use robotic arms built on the quadrotors in order to add new features to this flying machines. By using both robotic structures, new applications could be developed like collaborative tasks to move objects by pincers, track object with a camera in the end-effector as it is described in Allen et al. [1993] or anchoring the quadrotors to recharge its batteries.

This thesis develops 6DOF model for a quadrotor that includes a model of the perturbation of the robotic arm. Also design a nonlinear model predictive control to compensate the perturbations due the arm.

Chapter 3

Case Study Description and Control Problem

In this section, a full description of the dynamic equations of the quadrotor and its model is done. Also, the Newton-Euler solution for the particular case of the selected arm is detailed. Finally the description of the designed NMPC is presented at the end of this chapter.

3.1 Quadrotor Description

3.1.1 Dynamic Equations of a X-Type Quadrotor

The mathematical model of the quadrotor comes from the description done by [Pounds et al. \[2006\]](#). Let's suppose two frames as in Figure 3.1:

1. Inertial frame: $I = \{E_x, E_y, E_z\}$ where E_z is in the gravity direction.
2. Body frame: A frame located in the body of the quadrotor. Its axis are denoted by $A = \{E_1^a, E_2^a, E_3^a\}$, with center in $\xi = \{x^c, y^c, z^c\}$ in [m].

Both frames are related by a rotation matrix $R : A \rightarrow I$

It is defined $V(t)$ [m/s] and $\Omega(t)$ [rad/s] as the linear and angular velocity of the frame A expressed with respect to base A.

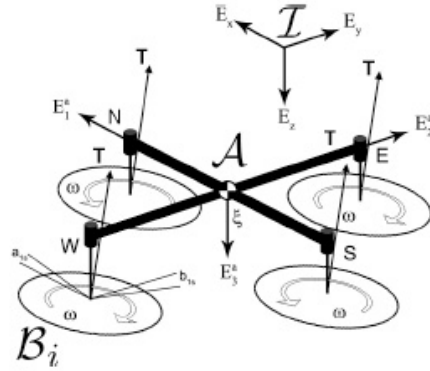


FIGURE 3.1: Blade system reference

The dynamic equations of the quadrotor are:

$$\dot{\xi}(t) = RV(t) \quad (3.1)$$

$$m\dot{V}(t) = -m\Omega(t) \times V(t) + mgR^T E_3^a + \sum_{r=1}^4 T(t)_r \quad (3.2)$$

$$\dot{R}(t) = Rsk(\Omega(t)) \quad (3.3)$$

$$I\dot{\Omega}(t) = -\Omega(t) \times I\Omega(t) + \sum_{r=1}^4 [Q(t)_r + M(t)_r] \quad (3.4)$$

$$T_r(t) = C_T \rho A_r r_r^2 \omega(t)_r^2 \begin{pmatrix} -\cos(b1s_r) \sin(a1s_r) \\ \sin(b1s_r) \\ -\cos(a1s_r) \cos(b1s_r) \end{pmatrix} \quad (3.5)$$

$$Q(t)_r = C_Q \rho A_r r_r^3 \omega(t)_r |\omega(t)_r| E_3^a \quad (3.6)$$

$$M(t)_r = T(t)_r \times D_r \quad (3.7)$$

where m [kg] is the mass of the rotor, I [kg m^2] is the rotational inertia, ρ [kg/m^3] is the density of the air, g [m/s^2] is the acceleration due the gravity, r [m] is the rotor radius, A [m^2] is the rotor disc area, ω_r [rad/s] is the angular velocity of the r -th rotor, $sk(\Omega)$ is the skew-Symmetric matrix, and R is the rotation matrix, which is constructed by the yaw-pitch-roll = (φ, θ, ψ) Euler angles. Moreover D_r [m] is the rotor displacement from the flyer center of gravity (CoG) ($D_1 = (0, d, h)$, $D_2 = (0, -d, h)$, $D_3 = (d, 0, h)$ and $D_4 = (-d, 0, h)$ with d [m] and h [m] as a length and height respectively above the CoG of the rotor).

Additionally T_r [N] is the thrust from the r -th rotor, Q_r [Nm] is the torque from the r -th rotor, M_r [Nm] is the momentum due the displacement of the thrust relative to the CoG, C_T is the non-dimensional thrust coefficient, which is an experimental parameter that could vary slightly, and C_Q is the non-dimensional torque coefficient, which is another experimental parameter.

Finally $a1s_r$ [rad] is the longitudinal flapping coefficient and $b1s_r$ [rad] is the lateral flapping coefficient. These both parameters are related to the blade flapping effect which will be explained a few lines later.

Having said that, it is possible to determine the behavior of any type-X quadrotor by modifying the above mentioned parameters inside equations (3.1), (3.2), (3.3), and (3.4). To clarify the use of all the previously equations a brief description is presented next:

- Equation (3.1) relates the linear velocity of the CoG with the inertial frame and the body frame.
- Equation (3.2) shows that the sum of the forces applied on a quadrotor have to be proportional to its linear acceleration. The equation is splitted in three different components. First, is the force due the coriolis effect. Second, is the force because of the gravity. And finally, is the thrust generated by each rotor.
- Equation (3.3) allows to relate the Euler angles rates to the angular velocity of the inertial frame.
- Equation (3.4) express that the sum of the torques applied have to be proportional to its angular acceleration. As before, the final torque is explained by three elements. The first one, is the torque created by an inertial system that is rotating

around an axis. Secondly, Q_i corresponds to the torque generated by each rotor due its angular velocity. Finally, $M(t)_i$ is the momentum created by the difference between the thrust of one of the rotors and the thrust generated by the opposite rotor.

- Equation (3.5) is generated by the angular velocity of the rotor. It depends on the geometry of the propellers and the density of the air, and is multiplied by a vector that modify the final direction of the thrust. Instead of a vertical direction, it appears a component on E_1^a and E_2^a due to the flapping blade effect (see equations (3.8), (3.9), (3.10)).
- Equation (3.6) is the torque generated by a mass (propeller) rotating around an axis (rotor).
- Equation (3.7) is generated because the thrust is not applied in the CoG and therefore a torque appears in the frame of the quadrotor.

The quadrotor can move in the three axis by combining the thrust and the torque of each rotor:

Move forward-backward: To move forward or backward it is necessary to make a difference between the thrust generated by the front rotor and the back rotor as it is represented in Figure 3.2. By this process the $\sum_{i=1}^4 M_i$ is not zero so the quadrotor has a slight torque that rotates the system until the forces and torques are balanced again. A pitch angle is then generated, which changes the direction of the thrust. A new component of force appears towards E_a^1 axis that allows an acceleration and therefore a velocity.

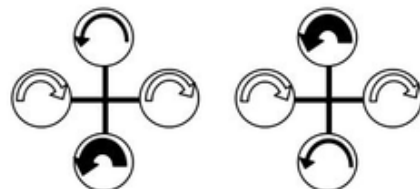


FIGURE 3.2: Forward-Backward movement

Move left-right: As it is shown in Figure 3.3, in order to accomplish these movements, it is necessary to create a difference between the thrust generated by the lateral

rotors. With the same concept explained before, a new torque is generated and the quadrotor bends a roll angle. Finally the thrust is splitted in a vertical component and in a component in the E_a^2 axis.

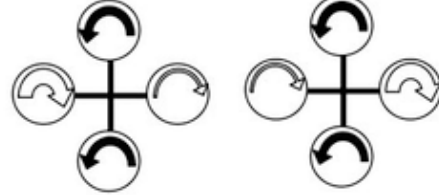


FIGURE 3.3: Left-Right movement

Move up-down: This movement is described in Figure 3.4. To move up or down it is necessary that the sum of all vertical thrusts component is more (up) or less (down) than the gravity force.

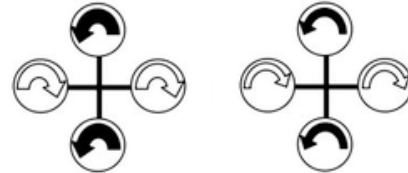


FIGURE 3.4: Up-Down movement

Rotate around E_a^3 (yaw motion): To rotate around the E_a^3 it should exist a torque around this axis. In a quadrotor, there are two motors that are rotating clockwise and two motors that are rotating counterclockwise in order to compensate the torque created by the rotation of each rotors as can be seen in Figure 3.5. Then, the only way to change the yaw angles is unbalancing the torques generated by each rotor when they are spinning. As it is possible to check in (3.6), the torque generated by the rotor is controlled by its angular velocity. So changing the velocity of the rotors it is possible to reach a determined yaw angle.

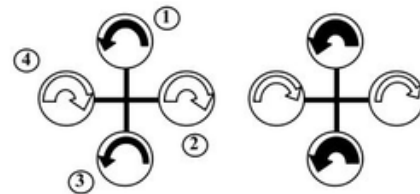


FIGURE 3.5: Rotate around E_a^3

By combining these four movements, it is possible to control the quadrotor position and its yaw angle. However, to the dynamics of the system, in order to keep the vehicle in a fixed position, pitch and roll angles must be minimized to zero, as on the contrary they generate a deviation of the thrust producing a motion in E_a^1 and E_a^2 .

Moreover, the blade flapping effect also could change the vertical thrust and make new components in the E_a^1 and E_a^2 . As it can be seen in Figure 3.6, front side of the rotor disk is called the advancing side, and the back side is called the retreating side. Blade flapping occurs when the rotors translate horizontally. In this case, a different lift between the advancing and retreating blades appears causing the rotor tip path plane to tilt. In order to modeling this effect it should be solved the constant and sinusoidal components of the blade centrifugal aerodynamic weight so that find the tilt angle of the plane as it is explained in ([Hussein](#)).

The flapping of the rotor is found by calculating the magnitude and direction of the rotor's translation. It is necessary to define a new local reference frame located in the rotor and aligned in the direction of the rotor's movement (B_i) as described in ([Pounds et al. \[2006\]](#)).

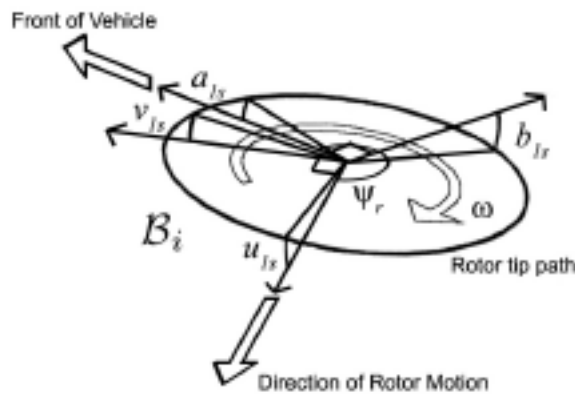


FIGURE 3.6: Parameters of a blade

In this frame, the longitudinal and lateral flapping angles (u_{1s_r}, v_{1s_r}) are calculated and now then expressed in the body frame of the quadrotor (a_{1s_r}, b_{1s_r}).

The expressions are the following:

$$v_{rr} = V(t) + \Omega(t) \times D_r \quad (3.8)$$

$$\mu(t)_{rr} = \frac{\|v(t)_{rr(1,2)}\|}{\omega(t)_r R} \quad (3.9)$$

$$\Psi(t)_{rr} = \arctan\left(\frac{v(t)_{rr(2)}}{v(t)_{rr(1)}}\right) \quad (3.10)$$

Equation (3.8) denotes the velocity vector of the r rotor. It's calculated as the sum of the velocity of the quadrotor plus the velocity due to the angular rotation of the system. Equation (3.9) is the ratio between the magnitude of the advance velocity and the linear velocity of the blades, and called the advance ratio. Equation (3.10) is the azimuthal direction of motion. On the other hand, the longitudinal and lateral flapping angles in the local reference B_r are:

$$u(t)_{1s_r} = \frac{1}{1 - \frac{\mu(t)_{rr}^2}{2}} \mu(t)_{rr}^2 (4\theta_r - 2\lambda_r) \quad (3.11)$$

$$v(t)_{1s_r} = \frac{1}{1 + \frac{\mu(t)_{rr}^2}{2}} \frac{4}{3} \left(\frac{C_t}{\sigma} \frac{2}{3} \frac{\mu(t)_{rr} \gamma}{a} + \mu(t)_{rr} \right) \quad (3.12)$$

$$\lambda_r = \sqrt{\frac{C_T}{2}} \quad (3.13)$$

$$\gamma = \frac{\rho a c r_r^4}{I_b} \quad (3.14)$$

Where σ is the rotor solidity which is the ratio between the total blade area and the total disk area, a is the blade slope gradient; c is the blade chord [m], r_r is the rotor radius [m]; I_b is the rotor blade rotational inertia of the flapping hinge [kg m^2].

Equation (3.11) is the longitudinal flapping angle. Depends on the parameters of the blade and the inflow of the rotor.

Equation (3.12) is the lateral flapping angle. Depends on the geometry of the blade, the inflow of the rotor and the Lock Number which is defined in [Pounds et al. \[2006\]](#).

Equation (3.13) is an approximation of the inflow's rotor.

Equation (3.14) is the Lock Number which represents the ratio between the aerodynamic and the inertial forces on the blade.

All the last described parameters are related with the geometry of the blades. Once the longitudinal and lateral flapping angles are calculated in the local body frame of the rotor, are then transformed back into the quadrotor body frame using the frame mapping $J_{B_r}^A$.

$$J_{B_r}^A = \begin{pmatrix} \cos(\Psi_{rr}) & -\sin(\Psi_{rr}) \\ \sin(\Psi_{rr}) & \cos(\Psi_{rr}) \end{pmatrix} \quad (3.15)$$

Finally, the influence of the pitch and roll rates are added to the flapping angles.

$$\begin{pmatrix} a1s_r \\ b1s_r \end{pmatrix} = J_{B_r}^A \begin{pmatrix} u_1s_r \\ v_1s_r \end{pmatrix} + \begin{pmatrix} \frac{16 \cdot \Omega_x}{\gamma \cdot \omega_r} + \frac{\Omega_y}{\omega_r} \\ \frac{1 - \mu_{rr}^2}{1 - \frac{\mu_{rr}^2}{2}} \\ -\frac{16 \cdot \Omega_y}{\gamma \cdot \omega_r} + \frac{\Omega_x}{\omega_r} \\ \frac{1 - \mu_{rr}^2}{1 - \frac{\mu_{rr}^2}{2}} \end{pmatrix} \quad (3.16)$$

with Ω_x and Ω_y as a pitch and roll rates, ω_r angular rate of the rotor r -th.

These values represent the effects of the geometry and physic properties of the propellers. Depending on the model and the blade shape used, the behavior of the system varies.

Also, by modeling this effect, it's possible to correct the non controlled lateral movement when the quadrotor is hover mode.

Still, the equations here presented are a mathematical approximation of a blade physics, where some assumptions have been made, all explained in [Johnson \[1994\]](#) and in [Bangura and Mahony](#).

Using the equations described on this section, the behavior of a quadrotor remains completely defined.

3.1.2 Dynamic Equations to Simulate the Real Plant

Once the NMPC solves the problem, the control signals that minimize the cost function are found. The framework of this study is limited to simulation scenarios so it's a model to emulate the real behavior for each sampled time, used also to obtain the variable states for the next optimization.

It must be noticed that the model used for the controller is different from the model used to simulate the real plant. For this reason it's possible to set the NMPC to absorb the potential errors and increase its robustness.

Subsequently, the model to emulate the behavior of the quadrotor with the arm it's a simplification of the real model described in Section 3.1.1. In this case, all the flapping effects will be removed from the dynamic equations.

$$a1s_r = 0$$

$$b1s_r = 0$$

which means that (3.5) has been modified as follows:

$$T_r(t) = C_T \rho A r^2 \omega(t)_r^2 \begin{pmatrix} 0 \\ 0 \\ -1 \end{pmatrix} \quad (3.17)$$

Usually, in a real environment, these values are calculated using an estimator with sensor fusion algorithms like it's described in Kis and Lantos [2011]. These techniques give an estimation of the state variables of the real system which are used to set the initial conditions of the NMPC algorithm for the next iteration. In Section 3.3.1 discretization of the model will be explained.

3.1.3 Physical and Geometrical Parameters of the Quadrotor Model

The equations defined in Section 3.1.1 are a parametrization of the behavior of the system.

To obtain a realistic behavior of the quadrotor is important to adjust the physical and geometrical parameters to real values. Focused on this aim, most of them have been taken from the quadrotor used by the researcher group that has motivated this study. This team has been working in a modification of the Pelican UAV from Ascending Technologies and its parameters can be found in its datasheet.

Other parameters used during this thesis come from the studies Bresciani and Gruene and Pannek [2011]. Some of them are experimental and the task to identify them was

out of the scope of this research, so they could not be verified. For this reason, these parameters are taken from other studies that have checked its authenticity.

Those parameters are split in several categories:

1. Physical: Gravity, viscosity and density of the air are defined to compute all physical equations.
2. Airframe: Its mass and inertial matrix have been defined in this section. Here we also explain the horizontal and vertical displacement from the rotors relative to CoG.
3. Rotor: All parameters about blade geometry and its physics are described in this category. Here is where all flapping blade effects are determined in function of the type of blade used by the quadrotor. Also its mass and its inertial matrix are detailed.
4. Constants: Some constants are precalculated to optimize the code during the control loop.

By changing the parameters and using the dynamic equations shown in Section 3.1.1, it is possible to simulate the behavior of any type of X-type quadrotor. The versatility of this method has allowed us to create an algorithm that is independent of the quadrotor used during the control process.

3.2 Robotic Arm Description

In this section the parameters and physics that define the behavior of the robotic arm will be detailed.

3.2.1 Dynamic Equations of a Robotic Arm

The aim of this section is to explain the dynamic equations of the robotic arm. First, it is necessary to explain the parametrization of the arm and then how to calculate the dynamic reaction on its base.

It is possible to modelize a robotic arm with serial joints by using the Denavit-Hartenberg parameters.

These four variables (also called DH parameters) define a particular convention about how to attach the reference frame of the links for a chain of joints.

This convention consists in assigning a coordinate frame to each link. For each joint there is a matrix transformation that allows changing from one frame to next. Concatenating this transformation matrix it is possible to relate the end-effector frame with the base frame. Depending of the type of joint (hinge or sliding), one of the four parameters is going to be the variable value and the other remain as constants.

The algorithm to select the right frames S_p and to fulfil DH parameters is:

1. The z -axis is in the direction of the joint axis. I.e. the rotation axis or the displacement axis.
2. The x -axis is the parallel to the common normal $x_p = z_{p-1} \times z_p$. The direction of x_p axis is from z_{p-1} to z_p .
3. The y -axis is selected to get the coordinated frame that accomplishes the right-handed rule.

The four parameters are:

d_p : Offset along previous z to the common normal. $Distance_{z_{p-1}}(S_{p-1}, z_{p-1} \cap x_p)$.

θ_p : Angle about previous z from old x to new x . $Angle_{z_{p-1}}(x_{p-1}, x_p)$.

a_p : Length of the common normal. For a revolute joint, it is the radius about previous z . $Distance_{x_p}(z_{p-1} \cap x_p, S_p)$.

α_p : Angle about common normal from the old z to new z . $Angle_{x_p}(z_{i-p}, z_p)$.

DH algorithm determines the configuration of the robotic arm and gives us an unambiguous description of the system. Knowing the angles of each joint it is also possible to exactly calculate the position and orientation of the end-effector relative to its base. This information will be important to estimate dynamic reactions into the base due to the motion of the end-effector. The final target that we want to reach is to obtain these

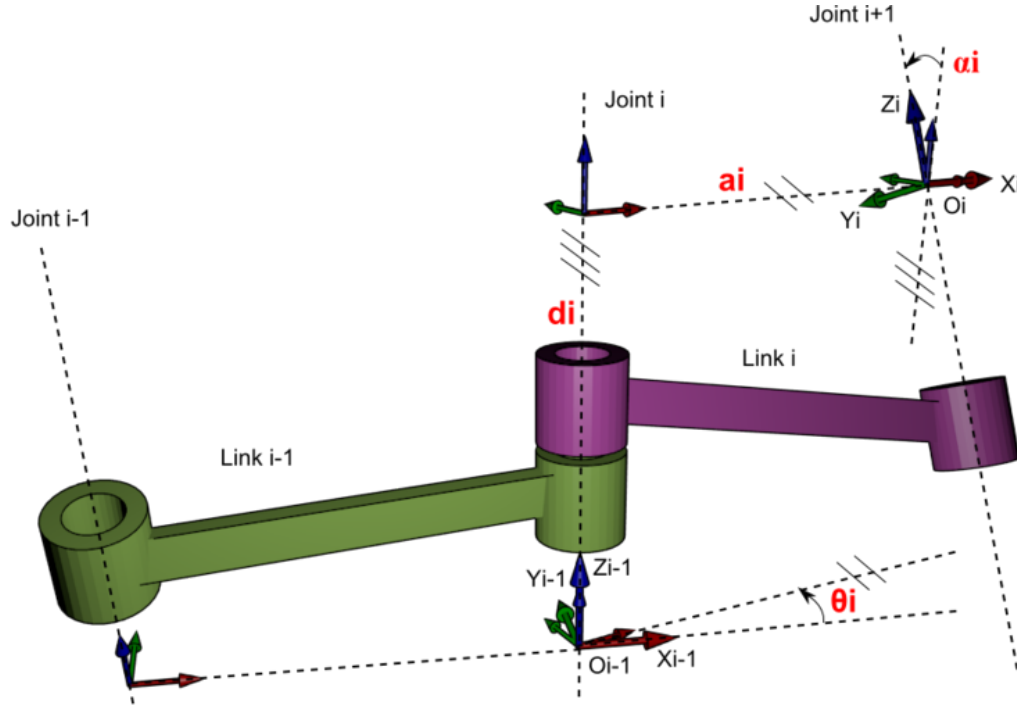


FIGURE 3.7: Denavit hartenberg parameters

forces and torques in order to couple them to the quadrotor as a perturbation. The method that has been selected to get the dynamic equations is Recursive Newton-Euler (RNE) algorithm applied into a robotic arm as it is explained in [Featherstone and Orin \[2000\]](#). RNE algorithm has two steps. The first step allows to calculate linear and angular velocity of each link by going from the base to the end-effector. The second step uses these velocities to solve dynamic equations and so being able to obtain the force and torque of each joint from end-effector to base. Finally, with this algorithm it is possible to get the reaction in the base due the motion of the system.

The formulation for the case of revolution joints is:

1. Forward step:

- Angular Velocity. The angular velocity of the frame k is:

$$\omega(t)_p = \omega(t)_{p-1} + \dot{q}(t)_p Z_{p-1} \quad (3.18)$$

where ω_{p-1} is the vector of the angular velocity of the previous frame, \dot{q}_p is the joint velocity and Z_{p-1} is the revolution axis.

- Angular Acceleration. The angular acceleration of the frame p is:

$$\dot{\omega}(t)_p = \dot{\omega}(t)_{p-1} + \dot{q}(t)_p^2 Z_{p-1} + \omega(t)_{p-1} \times (\dot{q}(t)_p Z_{p-1}) \quad (3.19)$$

where $\dot{\omega}(t)_p$ is the vector of the angular acceleration of the frame k and $\dot{q}(t)_p^2$ is the joint acceleration.

- Linear Velocity. The linear velocity of the frame k is:

$$v(t)_p = v(t)_{p-1} + (\omega(t)_p \times \Delta s_p) \quad (3.20)$$

where $v(t)_{p-1}$ is the linear velocity of the of the frame $p - 1$. The $\Delta s_p = d_p - d_{p-1}$ is the vector difference between the position of the frame $p - 1$ and the current frame p . Note that in order to calculate linear velocity it is necessary to have the angular velocity of the frame, so the order is mandatory.

- Linear Acceleration. The linear acceleration of the frame k is:

$$\dot{v}(t)_p = \dot{v}(t)_{p-1} + \dot{\omega}(t)_p \times \Delta s_p + \omega(t)_p \times (\omega(t)_p \times \Delta s_p) \quad (3.21)$$

where $\omega(t)_p \times (\omega(t)_p \times \Delta s_p)$ is the centrifugal acceleration. As same as before, in order to calculate linear acceleration it is necessary to have the angular acceleration.

Finally, to start the iteration, initial conditions have to be set:

$\omega_0(0)$: Initial angular velocity of the base.

$\dot{\omega}_0(0)$: Initial angular acceleration of the base.

$v_0(0)$: Initial linear velocity of the base.

$\dot{v}_0(0)$: Initial linear acceleration.

2. Backward step:

- Forces: Let's define a vector from the end of a link to its CoG $\Delta r_p = \bar{c}_p - d_p$ where \bar{c}_p is the location of the center of mass of link p .

The resulting force applied in the CoG is:

$$f(t)_p = f(t)_{p+1} + m_p [\dot{v}(t)_p + \dot{\omega}(t)_p \times \Delta r_p + \omega(t)_p \times (\omega(t)_p \times \Delta r_p)] \quad (3.22)$$

- Torques: First it has to be calculated the moment of the frame p .

$$n(t)_p = n(t)_{p-1} + (\Delta s_p + \Delta r_p) \times f(t)_p - \Delta r_p \times f(t)_{p+1} + D_p \dot{\omega}(t)_p + \omega(t)_p \times (D_p \omega(t)_p) \quad (3.23)$$

where D_p is the inertial tensor of link p in base space.

Once the moment is solved, the torque is computed as:

$$\tau(t)_p = n(t)_p^T Z_{p-1} + b_p \dot{q}(t)_p \quad (3.24)$$

where Z_{p-1} is the axis of the revolution and b_p is the viscous friction coefficient.

Once the backward step is finished the forces and torques of each joint are obtained and RNE algorithm is finished. Reaction force and reaction torque have been defined as follows:

Reaction force of the arm: The reaction force in the base is the force computed in the joint 1. $f_{ar} = f(t)_1$.

Reaction torque of the arm: The reaction torque in the base is the torque computed in the joint 1. $\tau_{ar} = \tau(t)_1$.

These reactions has been coupled in section 3.3.1.

3.2.2 Dynamic equations to Simulate the Real Robotic Arm

In order to implement the RNE algorithm using the DH parameters the Robotics toolbox from Corke [2011] has been used. This tool allow to use some methods to calculate the RNE algorithm or the acceleration of each joint given the current angles of the joints, their velocities and the torques desired. Also, it is possible to calculate the torque necessary to compensate the gravity effect.

To calculate the dynamic reactions of the base for each sampled time, it is necessary to have the angles, the velocities and the accelerations of each joint.

For the simulation model, a discretized method has been implemented. The method applied in this thesis to obtain the dynamic reactions is:

1. To calculate the Coriolis velocity using the current angles and velocities of the joints.
2. To estimate the necessary torque to be applied to each joint to compensate the effect of the gravity for the current position of the joints.
3. To compute the necessary torque to compensate the centrifugal force due the Coriolis effect.
4. To solve the direct kinematics using the current angles, velocities and the torques desired for each joint. This torques contemplate the enough torque to compensate the gravity and Coriolis effect, and also to achieve the motion planned. After solve it, the accelerations for each joint are obtained.
5. To update the joint velocity using the acceleration and the sampling time.
6. To update the joint angle using the velocity and the sampling time.
7. Finally, using the updated angles, velocities and accelerations, the RNE algorithm is applied. After this step, the base forces and torques reactions are obtained.

This algorithm is repeated for each sampled time. Due the complexity of the operations, it is an expensive method that spends a lot of CPU time. Once it is finished, the result is a vector with three forces and three moments (one per axis) represented in its base frame. This information will be used during the control loop as a perturbation of the system.

3.2.3 Physical and Geometrical Parameters of the Arm Model

There are some geometrical and physical parameters that define the dynamic model of the system.

The robotic arm used is designed by CSIC-UPC on collaboration with european project Arcas ([Sanramaria and Andrade \[2014\]](#)).

This arm is a prototype and its final design will be different from the model presented in this section.

However, the algorithm developed during this thesis are general and can be applied to any robotic arm. So, even if the arm changes, only by changing the physical and geometrical parameters the method explained in this study will work properly.

The system designed by CSIC-UPC has 6 joints set in different ways in order to reach to any orientation as it is represented in Figure 3.8.

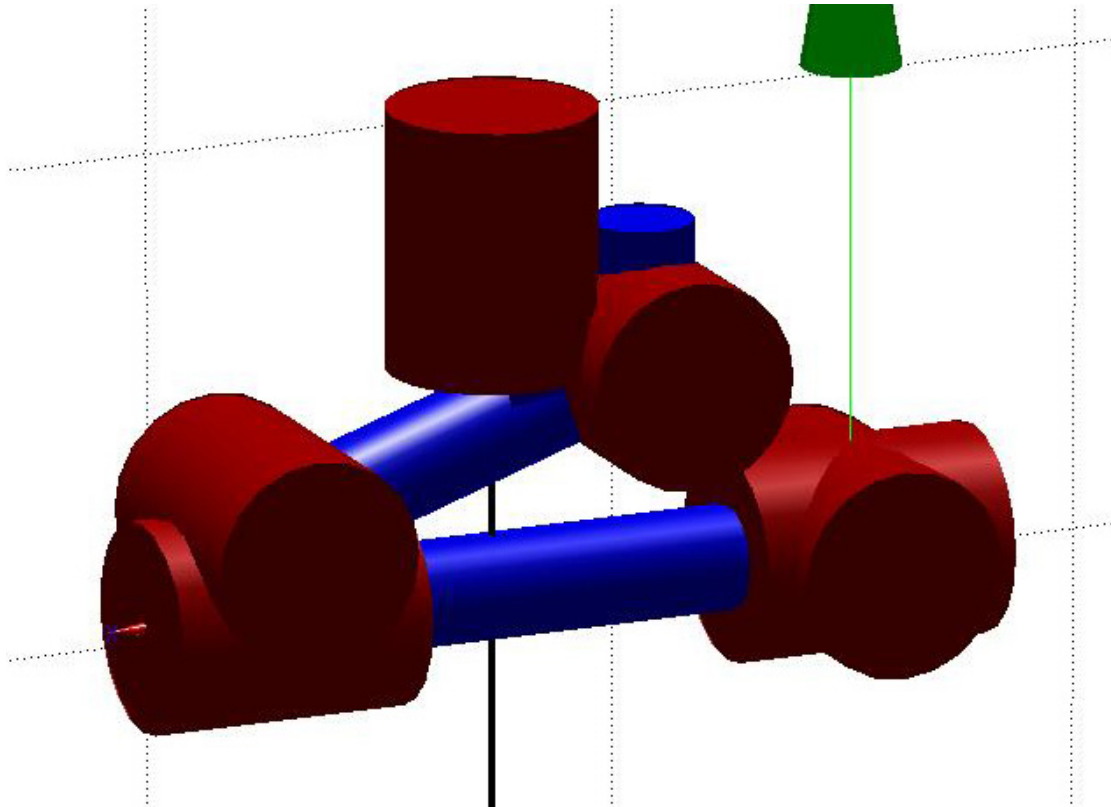


FIGURE 3.8: Matlab model of the robotic arm designed by CSIC-UPC.

The reference frame follows the same convention as the body frame of the quadrotor:

1. *x axis*: Aligned with the forward of the quadrotor.
2. *y axis*: Pointing to the floor (same direction as the gravity).
3. *z axis*: Completes the reference frame with the right-hand rule.

The first joint is to rotate the arm along $z - axis$ and move all the other articulations to any location of the xy plane . The next two joints move the rest of the chain in the xz plane. Finally, the last three joints are to orientate the end-effector independently of the other articulations.

During the simulation, the motion of each joint it is managed with a PID controller. The end-effector has a load of 0.05 kg to simulate that it is carrying an object.

To compute the Recursive Newton Euler algorithm it is necessary to know Denavit–Hartenberg parameters and the physical magnitudes of the system. All these values are taken from the original design of the arm done by CSIC-UPC. The next table (3.1) has all the DH parameters of the robotic arm used during the simulations.

TABLE 3.1: DH parameters of the robotic arm

Link i	a_i	d_i	α_i	θ_i
1	0.030	-0.026	$\pi/2$	q_1
2	0.079	0	0	$q_2 + \pi + 0.325$
3	0.0158	0	$\pi/2$	$q_3 + \pi - 0.325$
4	0	-0.118	π	q_4
5	0	0	$-\pi/2$	q_5
6	0	0	0	$q_6 + \pi/2$

3.3 NMPC Problem Statement

The NMPC algorithm is able to anticipate future events by using a dynamic model of the plant, and compute the optimal control to minimize the cost function subject to some restrictions as it is detailed in Section 2.3.

This algorithm has the following parts:

Optimization Problem: It is the formalization of the problem to solve. It relates the dynamic model, the cost function and the constraints. It defines the problem and its features. (Section 3.3.4).

Dynamic model: It is the internal model of the NMPC. This model is used to estimate the output of the real system given certain inputs. It defines the behaviour of the real plant. (Section 3.3.1).

Objective function: It is the function to be minimized. Describes the trajectory and the performance of the state variables. (Section 3.3.2).

Constraints: It is the restrictions to solve the optimization problem. Defines the limits of the state space and the region of the control signals. (Section 3.3.3).

3.3.1 Dynamic model

To control the system through a NMPC it is necessary to have an accurate model of the plant. The equations presented in Section 3.1.1 have been discretized and transformed into an algorithm to predict the behavior of the quadrotor.

To define a model the state variables and the control signals have to be defined:

$(x_1, x_2, x_3) = \xi(k) = (x(k), y(k), z(k))$: Position relative to the inertial frame.

$(x_4, x_5, x_6) = n(k) = (\psi(k), \theta(k), \varphi(k))$: Euler angles (yaw, pitch, roll).

$(x_7, x_8, x_9) = V(k) = (V(k)_x, V(k)_y, V(k)_z)$: Linear velocity relative to the inertial frame.

$(x_{10}, x_{11}, x_{12}) = \Omega(k) = (\Omega(k)_x, \Omega(k)_y, \Omega(k)_z)$: Angular velocity of the body frame.

The control variables are the signals able to control the whole plant and change its state during the time. In this case, the controllable values are the angular rate of the rotors.

$(u_1, u_2, u_3, u_4) = u(t) = (\omega(k)_1, \omega(k)_2, \omega(k)_3, \omega(k)_4)$: Angular rate of each rotor.

The equations (3.1), (3.2) and (3.4) provide the derivative of the position, orientation and velocities, so in order to compute the state variables in a simulation environment it is necessary to discretize them.

The sampling time is the amount of time that the time advances for each step of the control horizon. If is too large, the dynamics of the system will occur faster than the NMPC could control. On the other hand, if the sampling time is too short, the future predicted is near of the current time and the inertia of the motion are not possible to be controlled.

So it is important to balance both parameters in order to have a far horizon of control but with a short sampling time to detect the dynamics of the plant.

Depending on the control mode, the control horizon could vary. These variations are because the dynamic effects could affect more or less according of the motion of the quadrotor and then it is necessary a larger or shorter horizon to stabilize the plant.

The discrete state variables have been obtained as follows:

1. Position:

$$\frac{\xi(k+1) - \xi(k)}{T_s} = RV(k) \quad (3.25a)$$

$$\xi(k+1) = (x^c, y^c, z^c)^T(k+1) = (x^c, y^c, z^c)^T(k) + RV(k)T_s \quad (3.25b)$$

2. Linear Velocity:

$$m \frac{V(k+1) - V(k)}{T_s} = -m\Omega(k) \times V(k) + mgR^T E_3^a + \sum_{r=1}^4 T(k)_r \quad (3.26a)$$

$$linAcc(k) = -\Omega(k) \times V(k) + gR^T E_3^a + \frac{1}{m} \sum_{r=1}^4 T(k)_r \quad (3.26b)$$

$$V(k+1) = (V_x, V_y, V_z)(k+1) = (V_x, V_y, V_z)^T(k) + linAcc(k)T_s \quad (3.26c)$$

linAcc: Linear acceleration.

3. Euler Angles:

$$\frac{n(k+1) - n(k)}{T_s} = W^{-1}\Omega(k) \quad (3.27a)$$

$$n(k+1) = (\psi, \theta, \varphi)^T(k+1) = (\psi, \theta, \varphi)^T(k) + W^{-1}\Omega(k)T_s \quad (3.27b)$$

W^{-1} : Is the inverse of the wronskian. This matrix transforms the Euler angles rates to angles rates of the inertial frame (See Figure 3.1).

4. Angular Velocity:

$$I \frac{\Omega(k+1) - \Omega(k)}{T_s} = -\Omega(k) \times I\Omega(k) + \sum_{r=1}^4 [Q(k)_i + M(k)_i] \quad (3.28a)$$

$$angAcc(k) = -I^{-1}\Omega(k) \times I\Omega(k) + I^{-1} \sum_{r=1}^4 [Q(k)_r + M(k)_r] \quad (3.28b)$$

$$\Omega(k+1) = (\Omega_x, \Omega_y, \Omega_z)^T(k+1) = (\Omega_x, \Omega_y, \Omega_z)^T(k) + angAcc(k)T_s \quad (3.28c)$$

angAcc: Angular acceleration.

5. Dynamic Equations:

$$T_r(k) = C_T \rho A r^2 \omega(k)_r^2 \begin{pmatrix} -\cos(b1s_r) \sin(a1s_r) \\ \sin(b1s_r) \\ -\cos(a1s_r) \cos(b1s_r) \end{pmatrix} \quad (3.29a)$$

$$Q(k)_r = C_Q \rho A r^3 \omega(k)_r |\omega(k)_r| E_3^a \quad (3.29b)$$

$$M(k)_r = T(k)_r \times D_r \quad (3.29c)$$

These equations allow to compute the position of the quadrotor for each sampled time. To couple the quadrotor and arm dynamics, the discretized equations (3.26) and (3.28) have to be modified:

$$\text{linAcc}(k) = -\Omega(k) \times V(k) + g R^T E_3^a + \frac{1}{m} \sum_{i=r}^4 [T(k)_r] + F_{ar}(k) \quad (3.30a)$$

$$\text{angAcc}(k) = -I^{-1} \Omega(k) \times I \Omega(k) + I^{-1} \sum_{r=1}^4 [Q(k)_r + M(k)_r] + \tau_{ar}(k) \quad (3.30b)$$

The dynamic effects of the robotic arm are coupled by adding its reaction forces F_{ar} and its reaction torques τ_{ar} into the equations that compute the accelerations. In the Section 3.2 it is presented a full detailed explanation about how to obtain the reaction of the forces and torques of the arm.

The model is defined by the state variables as outputs, and the control signals as inputs of the system. By changing the rotors speed (control signals) it is possible to move the quadrotor to a desired position (state variables).

3.3.2 Objective function

The objective function, also called value function, is the expression that the NMPC should minimize by looking for the best control signals possible. This equation expresses the error to a specific state of the system. However, it does not represent the performance of the trajectory of the state variables. During this thesis, two different functions have been presented depending on if the quadrotor has to take off or if it has to reach a position and hold it.

So in this case, the objective function is the minimization of the error of some state variables. The matrix weights Q allows to prioritize which minimizations are more important than others. Also this matrix determines which variables are not going to be minimized. To use the prioritization system it should be done the normalization of the variables. By combining (3.34) and considering that the control signals have not been penalized, it was obtained the cost function used during the simulation:

$$\min_u J = \sum_{i=1}^N (x_d(k+i) - x(k+i|k)) Q (x_d(k+i) - x(k+i|k))^T \quad (3.31)$$

Notice that the desired vector of state variables is not dependent on the time because the goal remains constant in all simulated scenarios.

The state variables involved in the objective function are:

$$(x_1, x_2, x_3, x_4, x_9) = (x^c(k), y^c(k), z^c(k), \psi(k), V_z(k))$$

which are the quadrotor position, yaw and velocity in the z axis. On the other hand, pitch and roll are not included because if the system is forced to have a determined value of these states, it would imply that the quadrotor will move along its x or y axis.

As it was explained in Section 3.1.1, a tilt on its x or y axis generates a change of the direction of the thrust vector and a component of force could appear in the horizontal plane. So it is important to let free the pitch and roll in order to allow the appropriate movement of the quadrotor.

When the system moves along an horizontal axis, it is mandatory to increase the difference of the rotor speed between the two opposite rotors. By doing this, the total moment of the system is not compensated and starts to rotate in the z axis.

So it is necessary to fix the desired yaw angle to ensure that the system orientation is constant. If this restriction is not imposed, it is possible to move from one position to another but losing the orientation.

Nor linear nor angular velocity have been included due that it is impossible to hover a quadrotor if the system is not allowed to change its velocity conveniently (except the $V_z(k)$ which is forced to a value in order to take off). The matrix weighted weights are:

$$\text{for } m, n = 1, \dots, 12 \quad \begin{cases} Q(m, m) = \begin{cases} \frac{\gamma_{m,m}}{x_{m(ub)} - x_{m(lb)}} & \text{if } m = 1, 2, 3, 4, 9 \\ 0 & \text{otherwise} \end{cases} \\ Q(m, n) = 0 \end{cases} \quad (3.32)$$

where $\gamma_{m,m}$ is the weighted weight of the state variable x_m and $x_{m(ub)} - x_{m(lb)}$ is the range of the state variable x_m that it is used to normalize it. A more detailed description of the constraints it is presented in the Section 3.3.3. If the quadrotor has to take off $\gamma_{9,9} \neq 0$ otherwise $\gamma_{9,9} = 0$.

The NMPC uses this equation in order to find the optimal control signals and approach the system to its goals.

3.3.3 Constraints

The constraints define the state space of the problem. It is a polyhedric space where the NMPC has to find the optimal solution.

As bigger is this space, larger it is the search. So it is important to limit each variable with an upper and lower value. Also, if there are any linear or nonlinear relation between variables it should be implemented as a restriction.

The constraints limit all possible solutions to a set of them. Also, those restrictions allow to define the performance desired to accomplish its targets.

During this thesis, the constraints have been categorized in two types:

1. Constraints of the State Variables: All the restrictions related with the state variables are defined in this category. The upper and lower values have to be defined for the 12 state variables of the plant.
 - Position Bounds: It defines the volume allowed to move the quadrotor.

$$(x_{1ub}, x_{2ub}, x_{3ub}) = (x_{max}^c, y_{max}^c, z_{max}^c)$$

$$(x_{1lb}, x_{2lb}, x_{3lb}) = (x_{min}^c, y_{min}^c, z_{min}^c)$$

The trajectory of the quadrotor have to stay inside this volume in order to find a solution of the problem. Also, this volume has to be at least enough big to contain the possible error obtained during the hover maneuver.

- Euler Angles Bounds: It defines the maximum and minimum Euler angles allowed.

$$(x_{4ub}, x_{5ub}, x_{6ub}) = (\psi_{max}, \theta_{max}, \varphi_{max})$$

$$(x_{4lb}, x_{5lb}, x_{6lb}) = (\psi_{min}, \theta_{min}, \varphi_{min})$$

Taking into account that the $x_4 = \psi$ is the yaw angle, the range of this variable has to be enough wide to contain all the possible orientations in the xy plane necessary to accomplish the targets of the quadrotor.

On the other hand, the range of pitch ($x_5 = \theta$) and roll ($x_6 = \varphi$) angles have to be enough small to permit a slight tilt that allows to move the quadrotor but without losing the control of the plant. For large values of pitch or roll, the system can rotate completely until the thrust points to the same direction as the gravity, which would be critical for the plant. To avoid this, a small range has been chosen.

- Linear Velocity Bounds: It defines the maximum and minimum linear velocity allowed. These are referenced to the inertial frame.

$$(x_{7ub}, x_{8ub}, x_{9ub}) = (V_{xmax}, V_{ymax}, V_{zmax})$$

$$(x_{7lb}, x_{8lb}, x_{9lb}) = (V_{xmin}, V_{ymin}, V_{zmin})$$

Those constraints allow to smooth the behaviour of the quadrotor. Due the limit of its speed, the effect of its dynamics are less aggressive than for high speeds.

- Angular Velocity Bounds: Defines the range of the angular velocity of the quadrotor.

$$(x_{10ub}, x_{11ub}, x_{12ub}) = (\Omega_{xmax}, \Omega_{ymax}, \Omega_{zmax})$$

$$(x_{10lb}, x_{11lb}, x_{12lb}) = (\Omega_{xmin}, \Omega_{ymin}, \Omega_{zmin})$$

As before, it is important to define a narrow range of values in order to do not lose the control of the motion and avoid the possible problems with the

dynamic effects.

2. Constraints of the Control Signals: The restrictions of the control signals usually depends on the physics capabilities of the actuators. In this thesis the control signals are the angular rate of the rotors. So depending on the type of motor used, its limits and its behaviors could change.

The restrictions are:

- Angular Rates of the Rotors: It defines the range of the angular velocity of each rotor. The upper bound corresponds to the maximum possible angular rate that the motor is able to rotate.

These constraints take into account the sign of the value because the velocity could be positive or negative depending on if it turns clockwise or counter-clockwise.

$$u_{1ub} = \omega_{1max} > 0$$

$$u_{2ub} = \omega_{2max} < 0$$

$$u_{3ub} = \omega_{3max} > 0$$

$$u_{4ub} = \omega_{4max} < 0$$

On the other hand, the lower bound is the minimum value experimentally found to avoid lose the control of the system. Under this limit the quadrotor may fall down. So actually is not the minimum angular speed of the rotors.

$$u_{1lb} = \omega_{1min} > 0$$

$$u_{2lb} = \omega_{2min} < 0$$

$$u_{3lb} = \omega_{3min} > 0$$

$$u_{4lb} = \omega_{4min} < 0$$

So:

$$\omega_{1min} < u_1 < \omega_{1max}$$

$$\omega_{2min} < u_2 < \omega_{2max}$$

$$\omega_{3min} < u_3 < \omega_{3max}$$

$$\omega_{4min} < u_4 < \omega_{4max}$$

- Angular Accelerations of the Rotors: It defines the range of the angular acceleration for each rotor. It is important to define the maximum possible acceleration because this constraint limits how fast could change the angular speed of the rotors.

For wide ranges the maneuvers are faster but also more aggressive so the system could become uncontrolled.

On the other hand, for a narrow ranges, change the state variables of the plant could be too slow and then it may be difficult to accomplish its goals.

The maximum width of the ranges are determined by the physical properties of the rotor.

To implement this restriction it is necessary to know the last angular rate of the rotor and compute the current increment:

$$\Delta u_r(k) = u_r(k+i) - u_r(k+i-1) < \Delta u_{max} \rightarrow u_r(k+i) < \Delta u_{max} + u_r(k+i-1)$$

$$-\Delta u_r(k+i) = -u_r(k+i) + u_r(k+i-1) < \Delta u_{max} \rightarrow -u_r(k+i) < \max \Delta - u_r(k+i-1)$$

where Δu_{max} is the maximum increment of speed allowed and for $r \in [1,4]$.

Once all those constraints are applied, the states space of the system is defined and the optimizer can find the solution in the control space.

3.3.4 Optimization Problem

The Nonlinear Model Predictive Control algorithm is based on an iterative process which has to solve an optimization problem along a finite horizon.

The nonlinear system it is defined as:

$$\begin{cases} x(k+1) = f(x(k), u(k)) \\ y(k) = x(k) \end{cases} \quad (3.33)$$

The optimization problem that it has to be solved it is the following:

$$\min_u J = \sum_{i=1}^N (x_d(k+i) - x(k+i|k)) Q (x_d(k+i) - x(k+i|k))^T + \sum_{i=0}^{N_u-1} u(k+i) R u(k+i)^T \quad (3.34)$$

subject to:

$$y_{lb} < y(k+i) < y_{ub}, \quad i = 1, \dots, N \quad (3.35a)$$

$$u_{lb} < u(k+i) < u_{ub}, \quad i = 1, \dots, N \quad (3.35b)$$

$$-\Delta u_{max} < \Delta u(k+i) < \Delta u_{max}, \quad i = 0, \dots, N_u-1 \quad (3.35c)$$

$$\Delta u_{max}(k+i) = 0, \quad i = N_u, \dots, N-1 \quad (3.35d)$$

where $x(k+i|k)$ is the vector of the state variables, $x_d(k+i)$ is the vector reference of the state variables, the $u(t+k)$ is the control signal, $y(k+i)$ is the vector of measurements, Q is the weight matrix of the state variables, R is the weight matrix of the control signals, N is the prediction horizon length and N_u is the control horizon length. y_{lb} , y_{ub} , u_{lb} , u_{ub} and Δu_{max} are the constraints of the problem (more information in Section 3.3.3).

To choose an appropriate control horizon is important to control the plant. In order to simplify the algorithm, the length of the prediction horizon and the length of the control horizon are the same ($N = N_u$).

The horizon is the number of steps that the NMPC evolves the system toward the future to find the optimal control taking into account the future predictions. As the horizon increases, the complexity to solve the problem augments, and the CPU time required increases dramatically. So the power of CPU limits the horizon. If the control horizon is not enough large the dynamics of the system can not be predicted properly and then the control could be impossible.

The dynamic model has been defined in Section 3.3.1, the objective function has been presented in Section 3.3.2 and the constraints has been detailed in Section 3.3.3.

Chapter 4

Simulation Results

Some assumptions have been done in order to proceed to the simulations and validate the results:

Computational resources: It has supposed that the processor is powerful enough to compute all the operations in real time.

Accurate estimator of the state variables: It has assumed that there are a good filter that return an appropriate estimation of the 12 state variables. During these tests, this filter has been emulated by using a mathematical model of the quadrotor.

Point of application: It has assumed that the point of application of the forces and torques from the arm it has been in the origin of the body frame.

Control the angular rate of the rotors : It has supposed that it is possible to control the speed of the rotors. It has also assumed that their dynamics are instant.

Controlled environment: It has supposed a controlled environment, which means no extra perturbations.

The sampling time is constant: The frame rate of the loops has assumed constant.

Five scenarios have been prepared to test the algorithm developed during the thesis:

1. The quadrotor takes off and flies until reach to a specific altitude. The arm stays in a fixed position.

2. The quadrotor stays in a fixed position and the robotic arm stays in a fixed position. The aim of this test is to try if the system is able to keep a fixed position while its center of mass has changed.
3. The quadrotor stays in a fixed position and the robotic arm moves toward a target position. This scenario is a demonstration about how the NMPC compensates the dynamics of the arm due its motion.
4. The quadrotor moves toward a location and the robotic arm stays in a fixed position. The aim of this test is to show how the quadrotor can move to a fixed position while it is carrying an object that changes its center of mass.
5. The quadrotor moves toward a location and the robotic arm moves toward a target position. This situation has been prepared to check if the NMPC is able to predict the perturbations of the arm while the quadrotor it moves to a position.

During the next sections, a comparison between those modes are going to be presented. To obtain the perturbation it is necessary to simulate a motion of the arm. For these tests, the same arm motion are going to be applied in order to understand better the different behavior of the whole system. The arm could stay in a fixed position or move toward a specific pose. Each case has different reaction forces and torques.

Stays in a Fixed Position: The Figure 4.1 shows the fixed position of the arm.

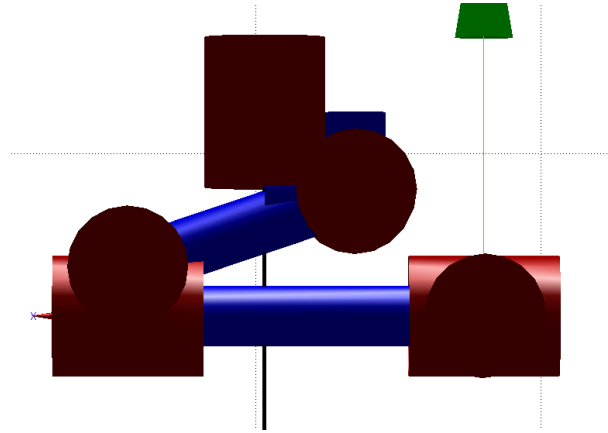


FIGURE 4.1: Arm robotic in the safe position

The plot showed in Figure 4.2 shows the reaction when the robotic arm stays in a fixed position. The forces and torques are constant during all the simulation.

Actually, the only remarkable force that is acting to the system is the force in the z axis which corresponds to the force of the gravity. Also, there is a slight moment in the y axis.

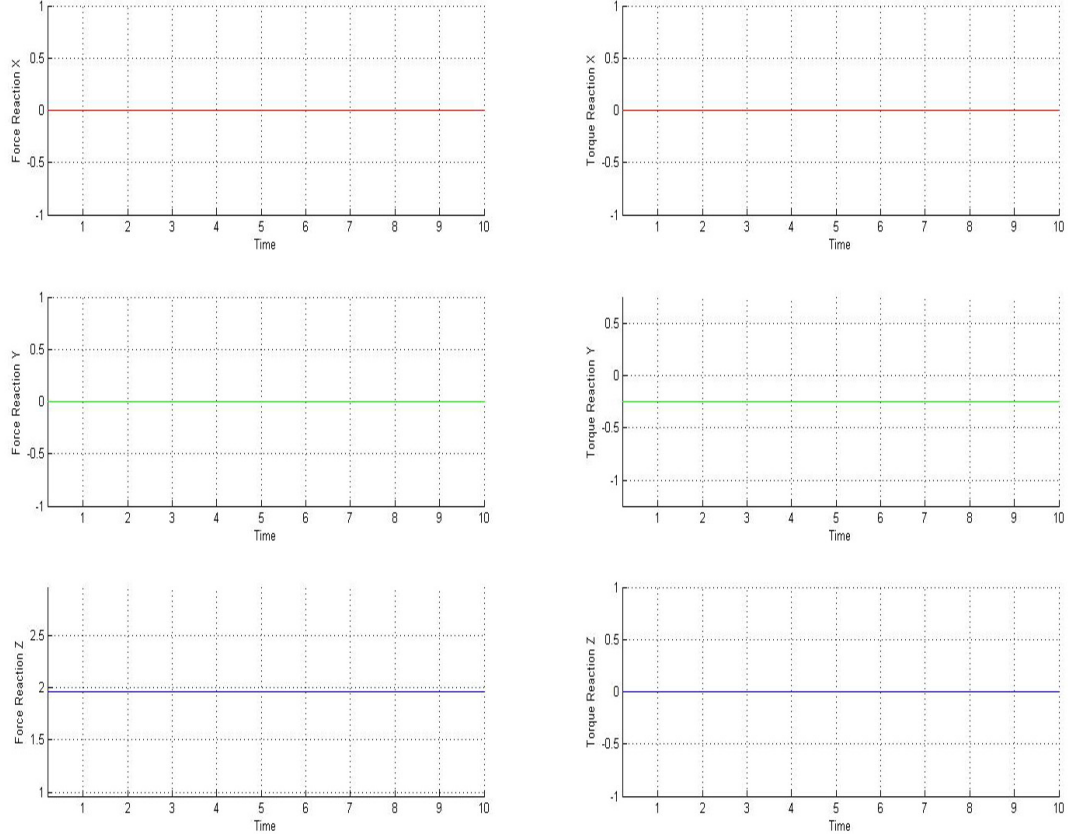


FIGURE 4.2: Dynamic Reaction in the base of the arm when remains in a fixed position

Moves to a Target Position: The movement consists in a small step of 0.2 [rad] in all the joints at the same time. The Figure 4.3 shows the reference of the movement and the trajectory of each joint.

The graphic of Figure 4.4 shows the forces that the quadrotor will receive when the robotic arm it moves. Those dynamics have to be controlled by the algorithm in order to reach to a steady state. The movement of the robotic arm starts after 3.4 seconds from the beginning of the simulation.

At the same time that the reference angles change, they appear the reaction of the force and torque. Once the position it is achieved, these dynamic effects disappear.

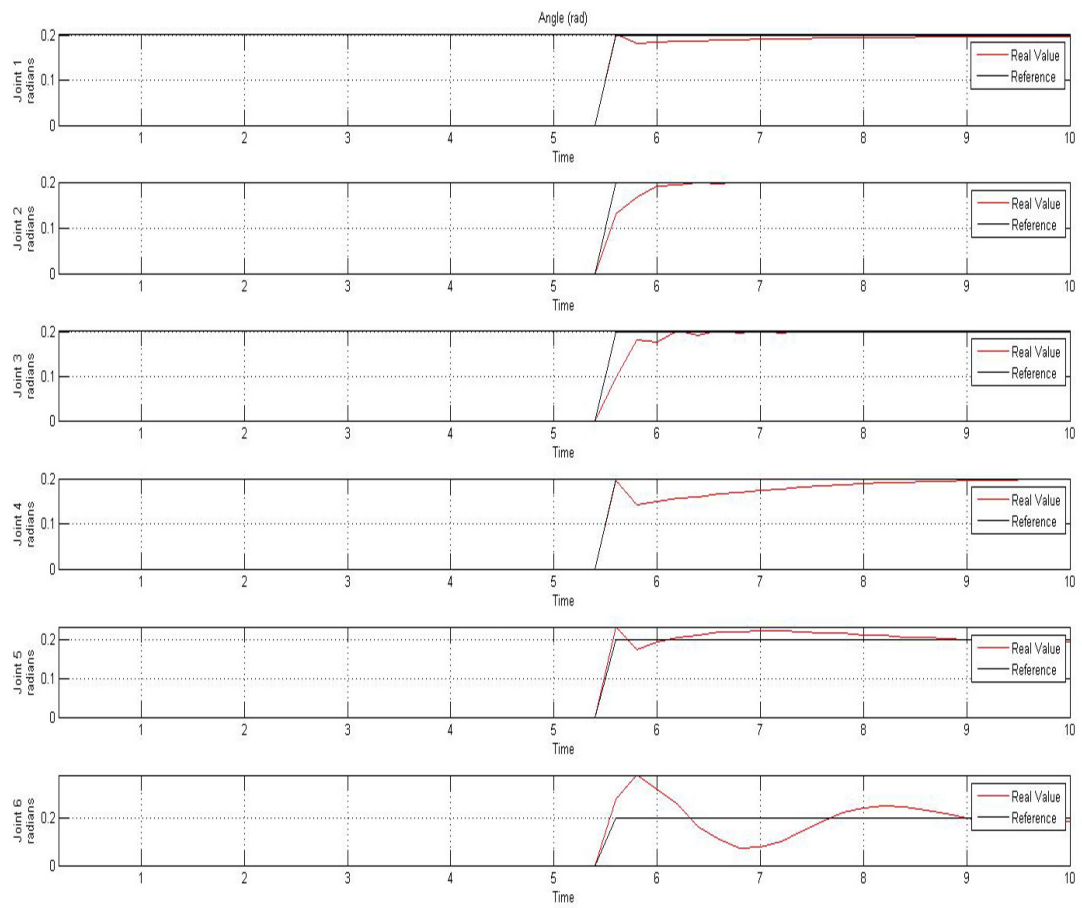


FIGURE 4.3: Reference and Angle of each joint

Depending on the scenario, the perturbations will change.

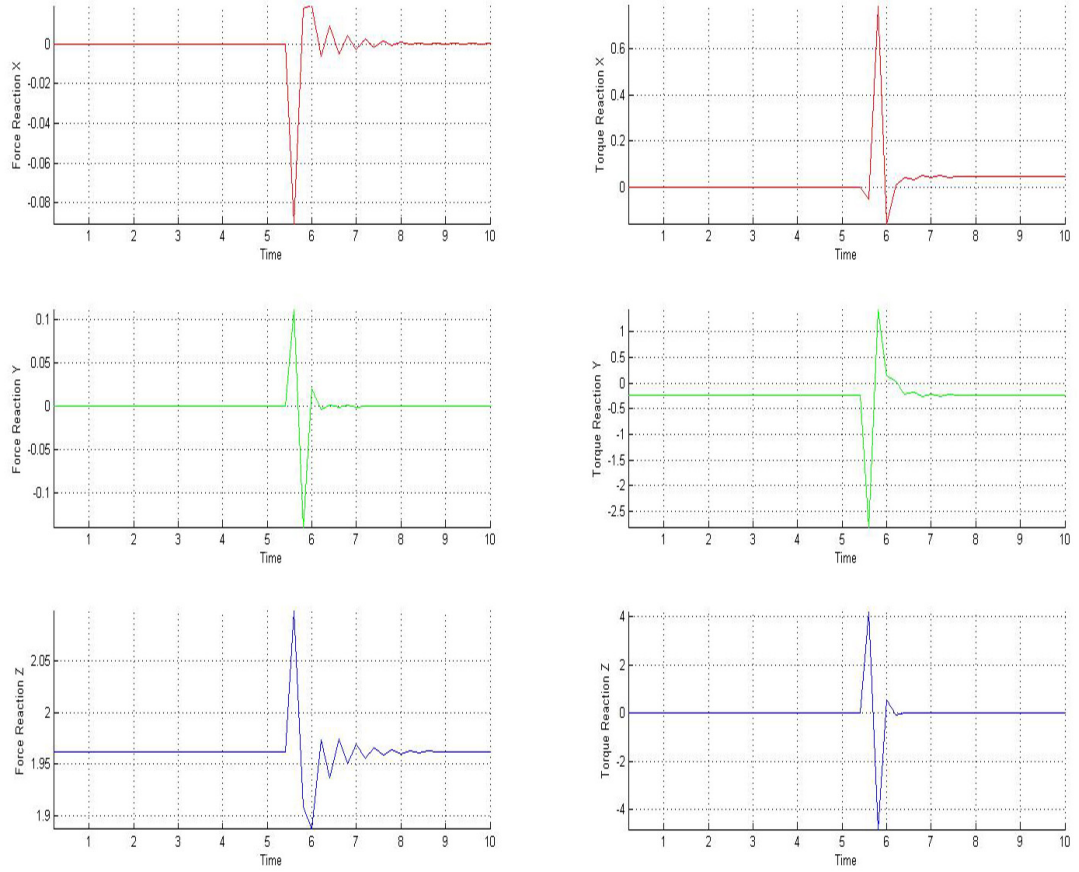


FIGURE 4.4: Dynamic Reaction in the base of the arm due its motion

4.1 Take off

The test consists in take off the quadrotor until reach a certain altitude. The robotic arm stays in a fixed position during all this maneuver. The whole system starts into the ground. The NMPC has to find the right combination of the inputs to take off. In this case, the matrix weights Q of the objective function (3.31) described in Section 3.3.2 changes depending on the altitude of the quadrotor:

- If the quadrotor is in the ground ($z^c(k) \leq 0$) the weights are:

$$Q(1, 1) = 0.1 \quad (4.1a)$$

$$Q(2, 2) = 0.1 \quad (4.1b)$$

$$Q(3, 3) = 0 \quad (4.1c)$$

$$Q(4, 4) = 2.5 \quad (4.1d)$$

$$Q(9, 9) = 0.1 \quad (4.1e)$$

- If the quadrotor starts to fly ($z^c(k) > 0$) the weights are:

$$Q(1, 1) = 0.1 \quad (4.2a)$$

$$Q(2, 2) = 0.1 \quad (4.2b)$$

$$Q(3, 3) = 0.025 \quad (4.2c)$$

$$Q(4, 4) = 2.5 \quad (4.2d)$$

$$Q(9, 9) = 0 \quad (4.2e)$$

with $Q(1, 1)$ the weight of the $x^c(k)$ position, $Q(2, 2)$ the weight of $y^c(k)$ position, $Q(3, 3)$ the weight of the $z^c(k)$ position, $Q(4, 4)$ the weight of the yaw ($\varphi(k)$) angle and $Q(9, 9)$ the weight of the $V_z(k)$ velocity.

By using this strategy, the NMPC forces the quadrotor to accelerate along the z axis until starts to fly. Once the quadrotor has the state variable $z^c(k) > 0$ will mean that has enough thrust to reach to the altitude desired, so the cost function changes to find the right location in the space. The prioritization of the cost function is, first of all, maintain the yaw orientation, then fix the position in the plane xy and finally move to a z desired.

TABLE 4.1: Initial Conditions for Take Off

Parameters	Value
Initial State Variables	[0, 0, 0, 0, 0, 0, 0, 0, 0, 0, 0, 0]
Desired State Variables	[0, 0, 4, 0, 0, 0, 0, 0, 0, 0, 0, 0]
Initial Control Signal	[200, -200, 200, -200]
Horizon Control	10
Sampling Time	0.2s
Simulation Time	10s

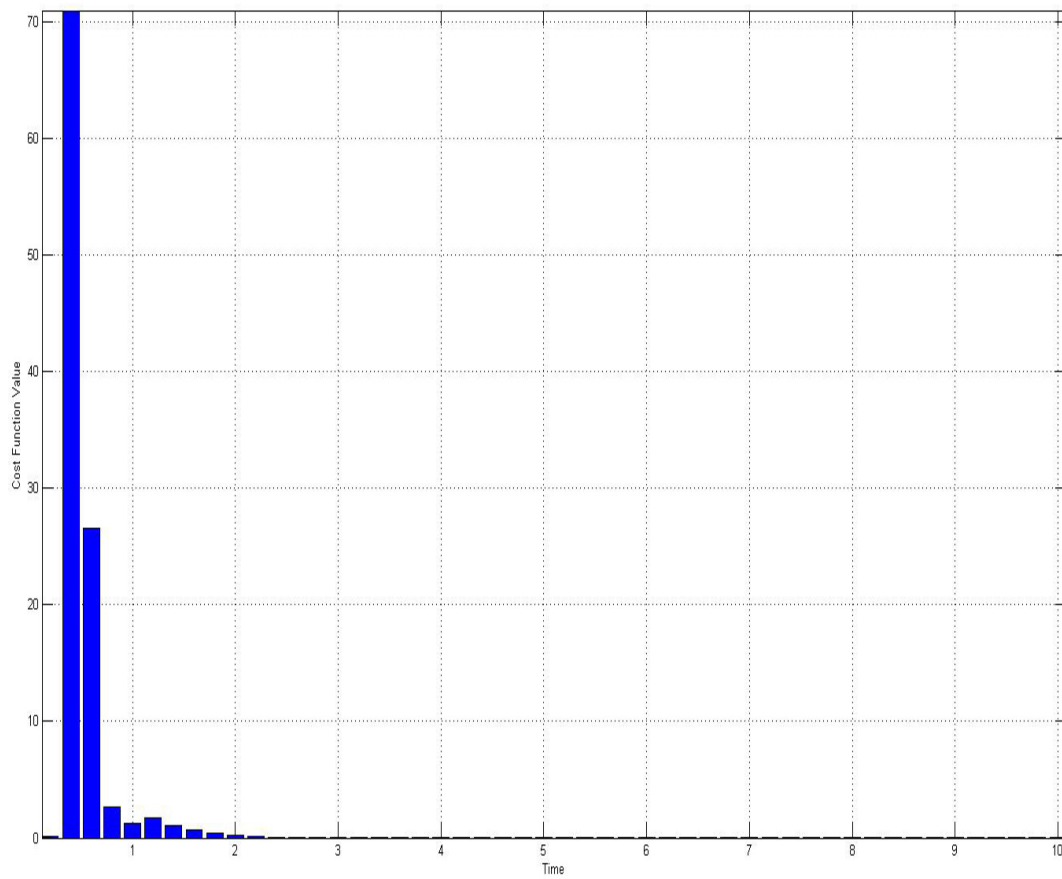


FIGURE 4.5: Cost function during the Take Off

As it is possible to see in Figure 4.5, there is a peak. Before this point, it is the step where the controller tries to force the quadrotor to move up. After this point is when the cost function has changed its branch, and the NMPC tries to bring the system to 4m from the ground.

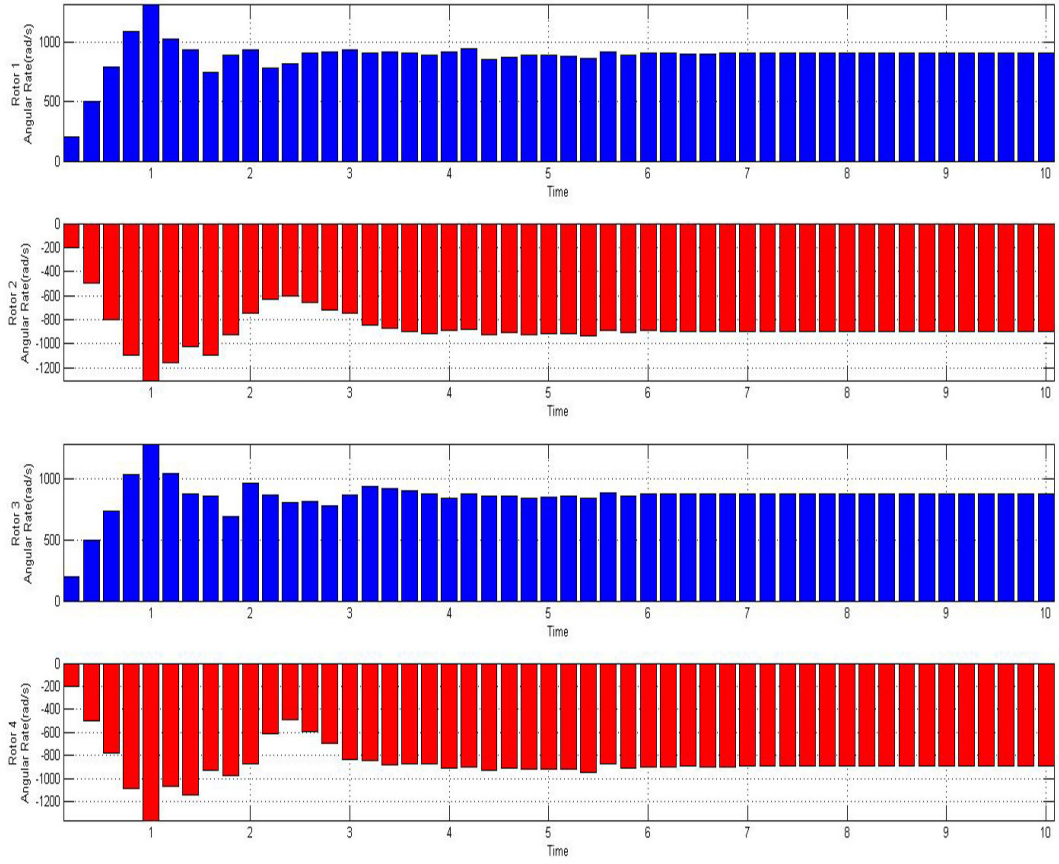


FIGURE 4.6: Control signal for a Take Off

As it is shown in Figure 4.6, at the beginning the angular rate of the rotors increase its value in order to accelerate the quadrotor. Once it is flying, the control signal is looking for the way to reach to a steady state. On the other hand, it is possible to observe the change of the behavior in the control signal when the quadrotor reaches to the desired position.

Finally, the performance of the motion could be observed in Figure 4.7.

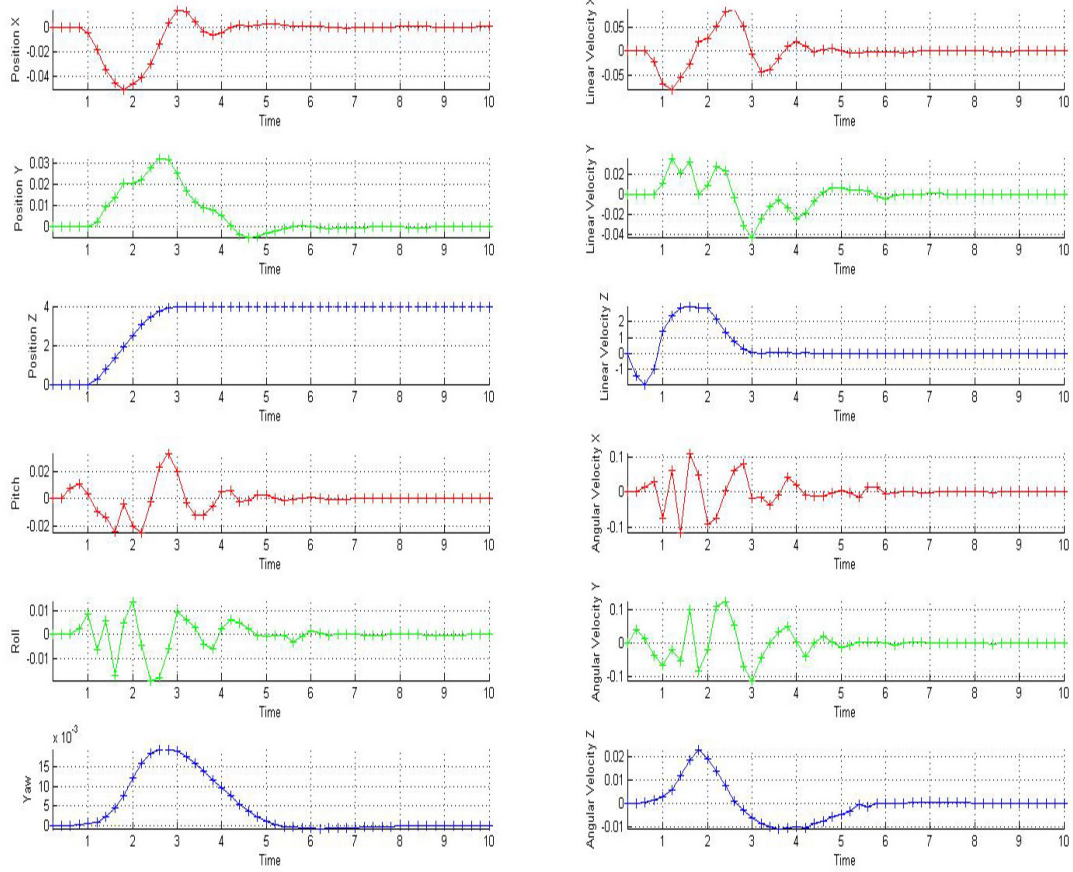


FIGURE 4.7: State variables for the Take off

Once the system has enough thrust to take off, it starts increasing its altitude until the 4m. At the same time it is compensating the movement in the xy plane and the tentative to change its yaw.

TABLE 4.2: Summary of Take Off

Parameters	Value
ISE	6.2
Maximum error	2.5
Time to reach to Steady State	3.2s

4.2 Quadrotor in a fixed position

The aim of this section is to try to stabilize the quadrotor in a fixed position and orientation in the space $(x^c(k), y^c(k), z^c(k), \varphi(k)) = (0, 0, 4, 0)$.

During these scenarios, the matrix weights are:

$$Q(1, 1) = 0.1 \quad (4.3a)$$

$$Q(2, 2) = 0.1 \quad (4.3b)$$

$$Q(3, 3) = 0.025 \quad (4.3c)$$

$$Q(4, 4) = 2.5 \quad (4.3d)$$

$$Q(9, 9) = 0 \quad (4.3e)$$

These weights assure that the quadrotor will stay near the position $(0, 0, 4)$ and with a fixed orientation.

At the beginning, the rotors start with an initial angular speed $(900, -900, 900, -900)$.

Those are the necessary velocities to avoid that the system falls.

TABLE 4.3: Initial Conditions for Static Control

Parameters	Value
Initial State Variables	$[0, 0, 4, 0, 0, 0, 0, 0, 0, 0, 0, 0]$
Desired State Variables	$[0, 0, 4, 0, 0, 0, 0, 0, 0, 0, 0, 0]$
Initial Control Signal	$[900, -900, 900, -900]$
Horizon Control	10
Sampling Time	$0.2s$
Simulation Time	$10s$

4.2.1 Robotic Arm in a fixed position

This is the simplest test where the robotic arm stays in a fixed position and the quadrotor has to compensate its perturbations.

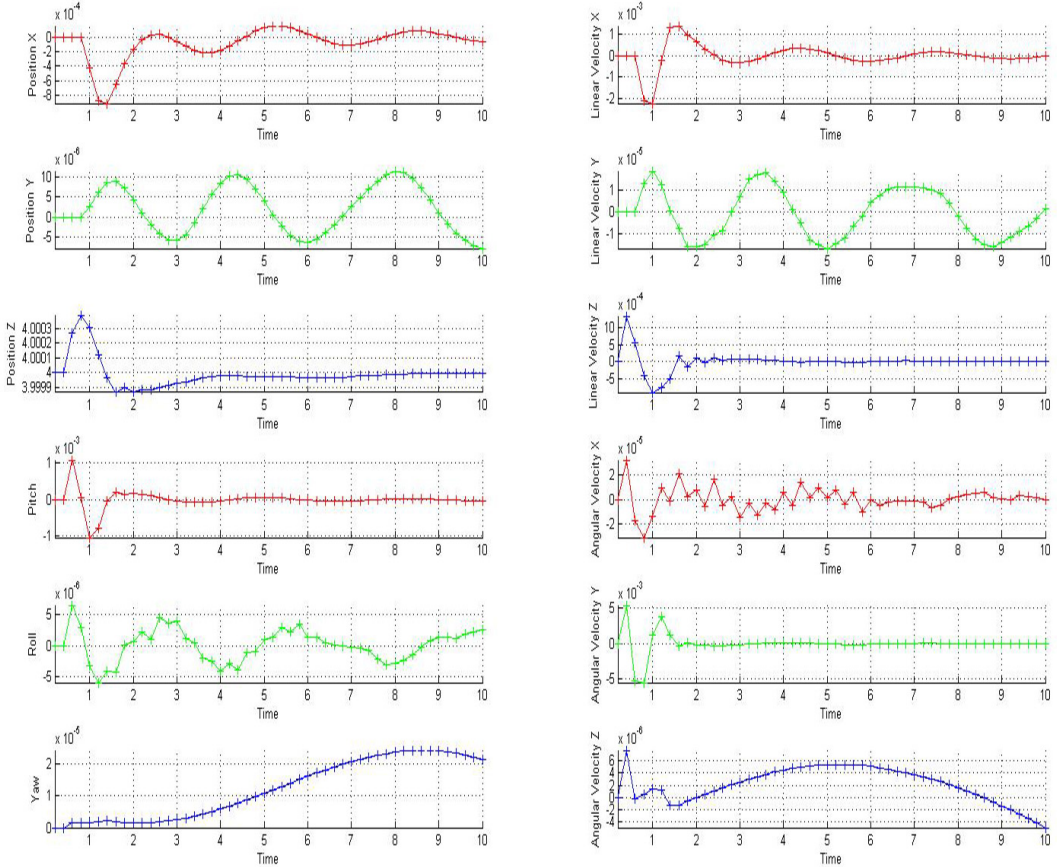


FIGURE 4.8: State variables for a quadrotor in a fixed position and an arm in a fixed position

As it is possible to see in Figure 4.8, the NMPC could find the steady state of the quadrotor and bring it to the desired state variables.

In order to compensate the moment generated by the arm, the four rotors have different speeds (911.2652, -894.7493, 877.9722, -894.7513). Notice that the forward and backward rotors are unbalanced while the left and right are rotating at the same velocity.

All the values are small enough to consider them as a noise. It is clear to see in Figure 4.8 how the velocity in the y axis is correcting the deviation in this axis.

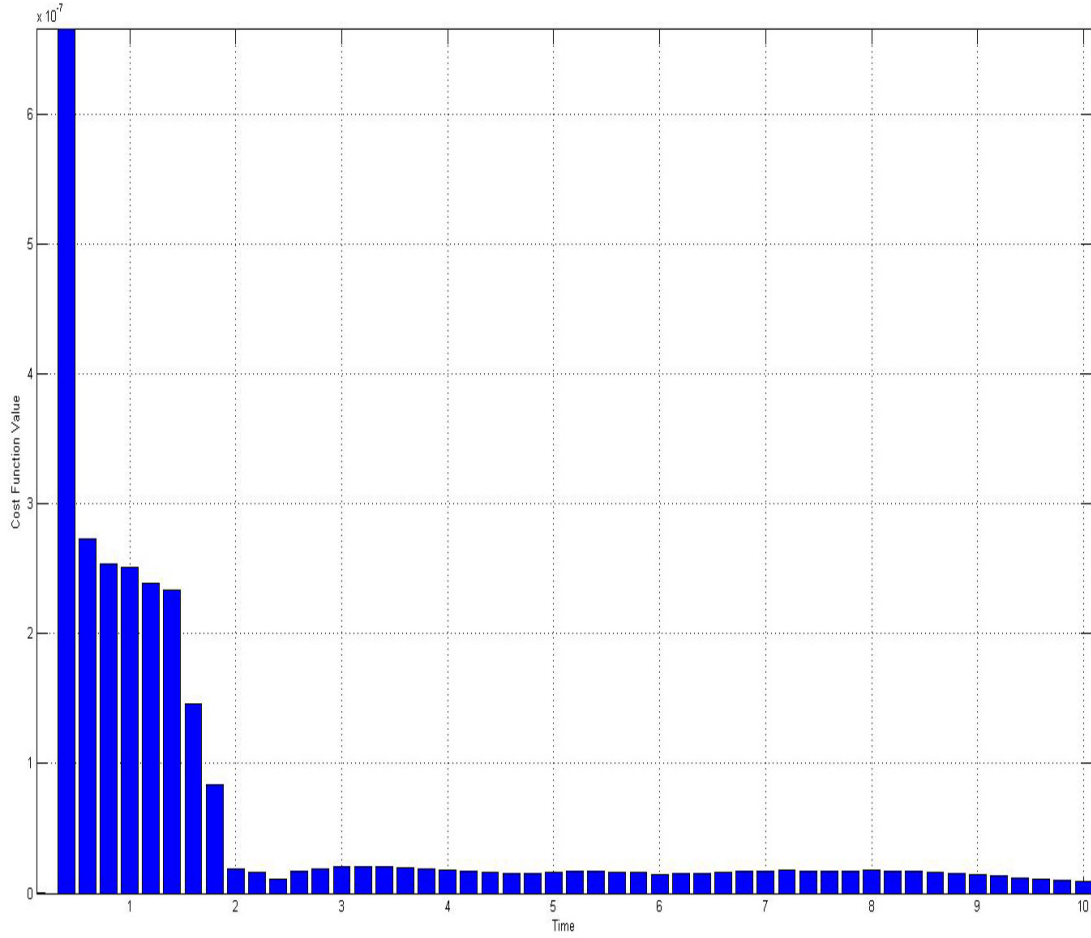


FIGURE 4.9: Cost function for a quadrotor in a fixed position and an arm in a fixed position

As it is possible to see in Figure 4.9, approximately after 2 seconds, the system finds the correct combination of the speed rotors to reach to a steady state. The first peak it is because the forces are unbalanced and the quadrotor moves slightly to up. Once the quadrotor is completely stable, it remains in a fixed position until the end of the simulation.

TABLE 4.4: Summary of the control for a quadrotor in a fixed position and an arm in a fixed position

Parameters	Value
ISE	$2.75e^{-6}$
Maximum error	$6.75e^{-7}$
Time to reach to Steady State	2.0s

4.2.2 Robotic Arm in movement

During this test, the perturbation of the robotic arm due its motion it has been applied to show its impact in the whole system.

The motion of the robotic arm starts at second 3.4 as it is possible to see in the figures 4.10 and 4.11. In that moment the forces and torques from the arm appear and destabilize the system.

In Figure 4.10 it is shown how for a few seconds the system loses its position. In the velocities graph it is possible to observe how the controller tries to stabilize the system by moving the quadrotor to compensate the perturbations.

As it is represented in Figure 4.11, there is a big peak. The error augments drastically when the dynamic effects of the arm are important enough to affect to the motion of the quadrotor.

This peak occurs when the arm suddenly changes its motion. Once the arm is stable, the NMPC could restore the position of the system.

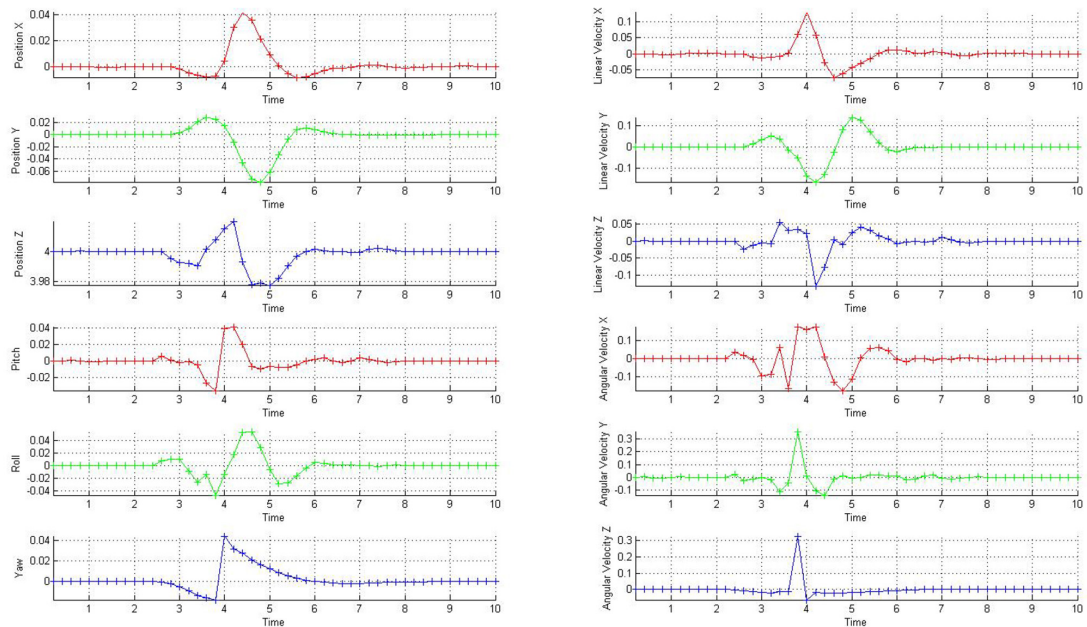


FIGURE 4.10: State variables for a quadrotor in a fixed position and an arm in movement

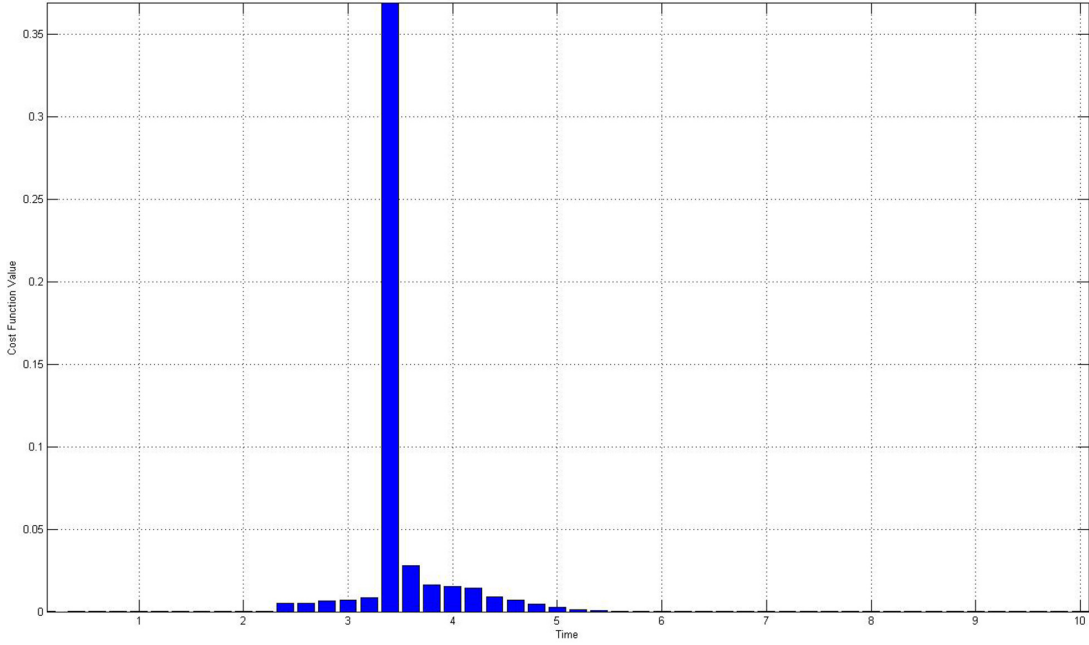


FIGURE 4.11: Cost function for a quadrotor in a fixed position and an arm in movement

TABLE 4.5: Summary of the control for a quadrotor in a fixed position and an arm in movement

Parameters	Value
ISE	0.5
Maximum error	0.37
Time to reach to Steady State	1.8s

4.3 Quadrotor in movement

The aim of this section is to try to carry the whole system from an initial position to a target position in the space.

During these scenarios, the weights of the objective function are the same as in (4.3). Again the prioritization of the cost function is to control yaw orientation, then xy position and finally move to a z altitude. The goal of the cost function is to move the quadrotor from the $(x^c(0), y^c(0), z^c(0), \varphi(0)) = (0, 0, 4, 0)$ to $(x^c(10), y^c(10), z^c(10), \varphi(10)) = (0.75, 0.75, 4, 0)$ and reach to a steady state in this position. The rotors start with an initial angular speed $(900, -900, 900, -900)[\text{rad/s}]$.

Finally, it has been necessary to increase the length of the control horizon. It has been increased because the movement of the quadrotor generates important dynamic effects that need more time to predict them and control them.

TABLE 4.6: Initial Conditions for the trajectory of the Quadrotor

Parameters	Value
Initial State Variables	[0, 0, 4, 0, 0, 0, 0, 0, 0, 0, 0, 0]
Desired State Variables	[0.75, 0.75, 4, 0, 0, 0, 0, 0, 0, 0, 0, 0]
Initial Control Signal	[900, -900, 900, -900]
Horizon Control	12
Sampling Time	0.2s
Simulation Time	10s

4.3.1 Robotic Arm in a fixed position

In this scenario, the quadrotor moves to a position while the robotic arm stays immobile.

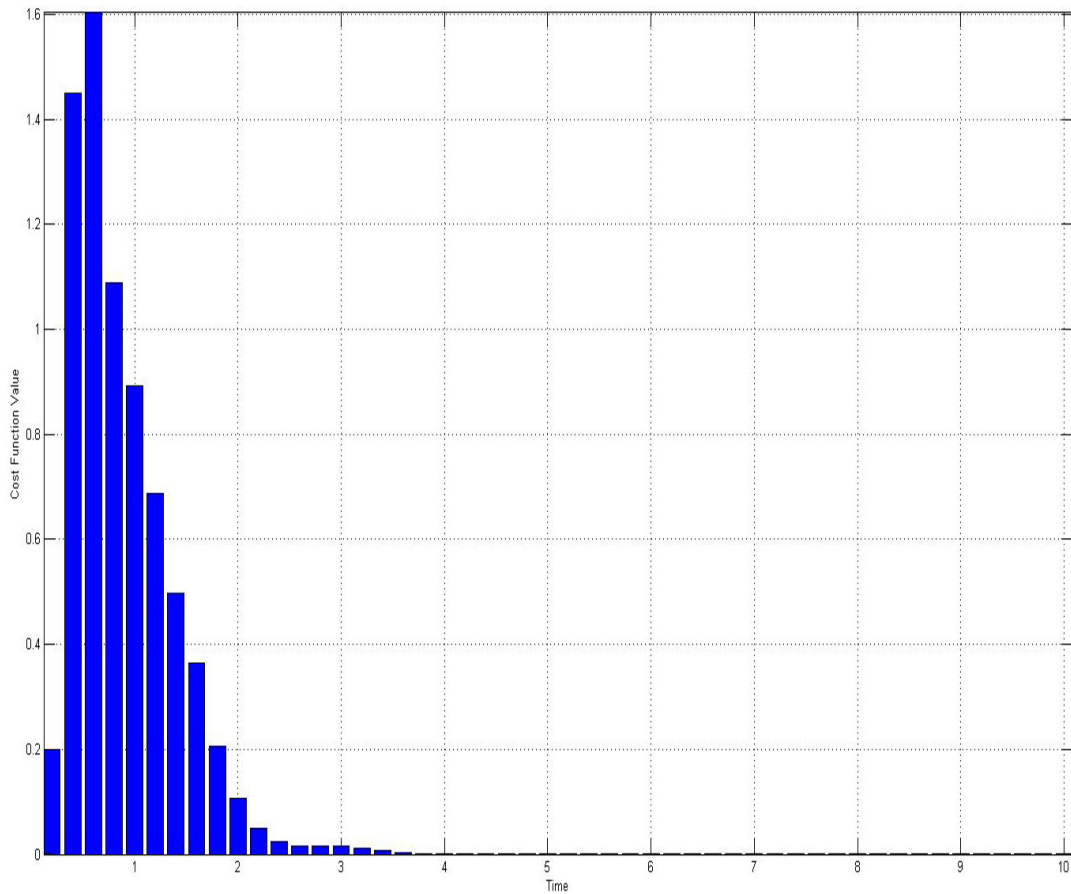


FIGURE 4.12: Cost function for a quadrotor in movement and an arm in a fixed position

The peak shown in Figure 4.12 corresponds to the maximum error. This value appears because the system changes its altitude when it is moving to the desired position. The change of its altitude is because two different factors:

1. The system does not start from a stable position. The initial values of the speed rotors are not the values that maintain the quadrotor in a fixed position. So the NMPC searches the right approach to reach to the steady state around the altitude desired.
2. The system has as a priority maintain the yaw orientation all the time.

Then the NMPC tries to keep the orientation of the quadrotor and move it toward a position but using the prioritization explained before, which means that the worst performance will be in the z altitude control.

The quadrotor it approaches to its target at each sampled time so the value of the cost function is decreasing as it is shown in Figure 4.12.

The Figure 4.13 shows the performance of the system. The target position x and y is reached with a slight peak. Also, it is possible to see how the effect of the movement implies a modification of the z position as explained above.

On the other hand, is possible to observe that to move in the xy plane, a tilt in roll and pitch it is necessary.

TABLE 4.7: Summary of the control for a quadrotor in movement and an arm in a fixed position

Parameters	Value
ISE	7.25
Maximum error	1.6
Time to reach to Steady State	3.75s

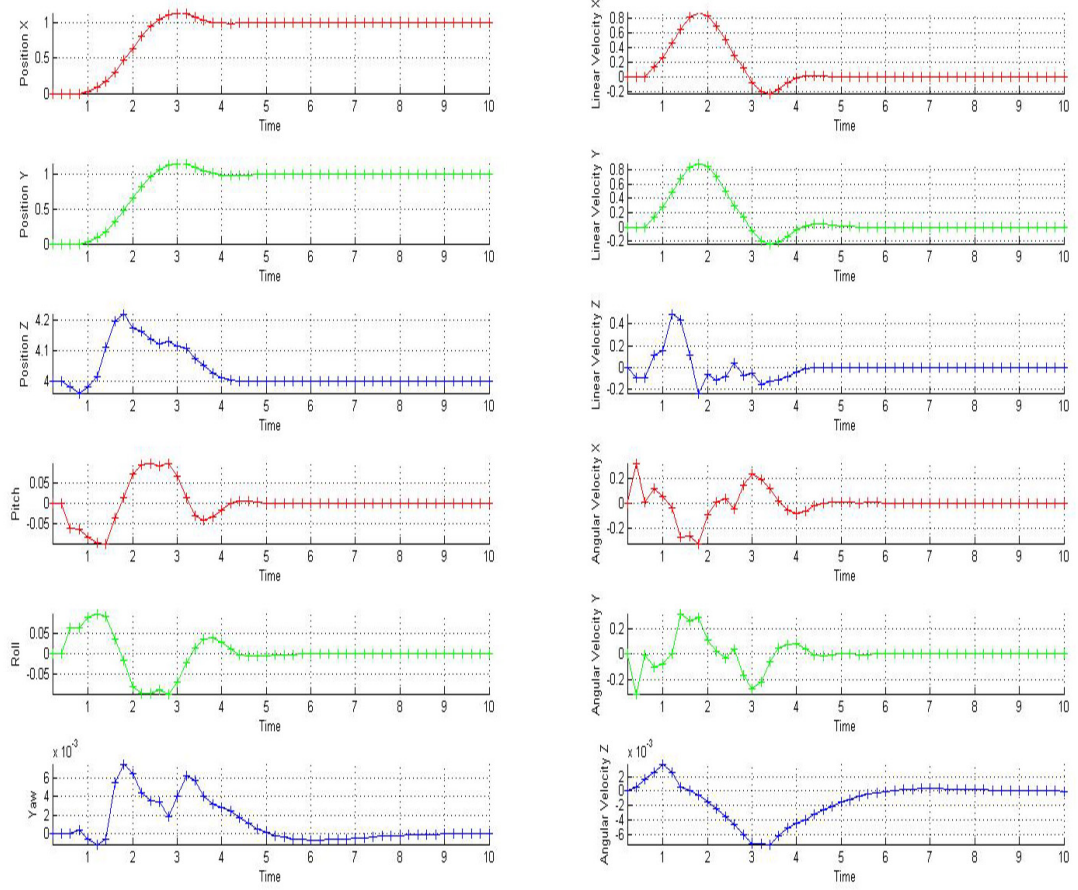


FIGURE 4.13: State variables for a quadrotor in movement and an arm in a fixed position

4.3.2 Robotic Arm in movement

Finally, the last case is to analyse how the perturbations from the robotic arm affects to the quadrotor while it is moving.

Figure 4.14 shows the cost function during the simulation. The first part is the error due the distance to the target position. At second 3.4 starts the movement of the arm and appears a second peak. This second part perturbs all the system and increases drastically the error. Actually, when the robotic arm starts to move, the quadrotor is in steady state so the response of the system is fastest than the activation of the arm.

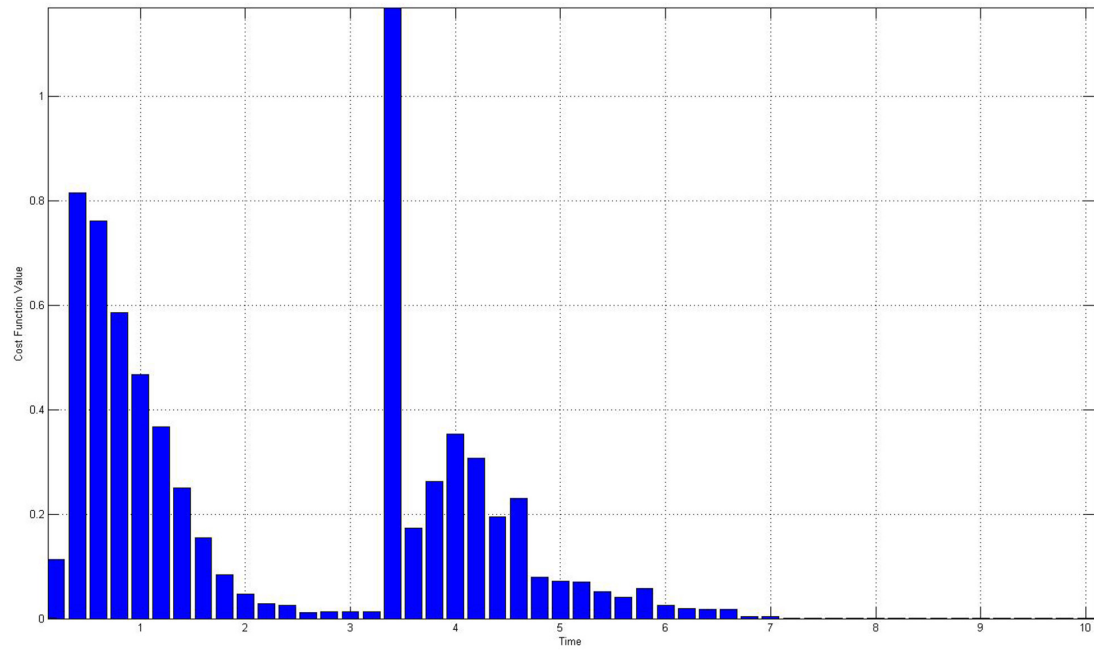


FIGURE 4.14: Cost function for a quadrotor in movement and an arm in movement

Figure 4.14 presents the behaviour of the system. The quadrotors moves toward the target position and reaches the steady state. It is possible to observe that the position and orientation change when the perturbation starts. In the yaw graph appears a peak at 3.4 seconds that corresponds the beginning of the arm motion. Once the movement of the arm ends, all the variables reach the steady state before the end of the simulation.

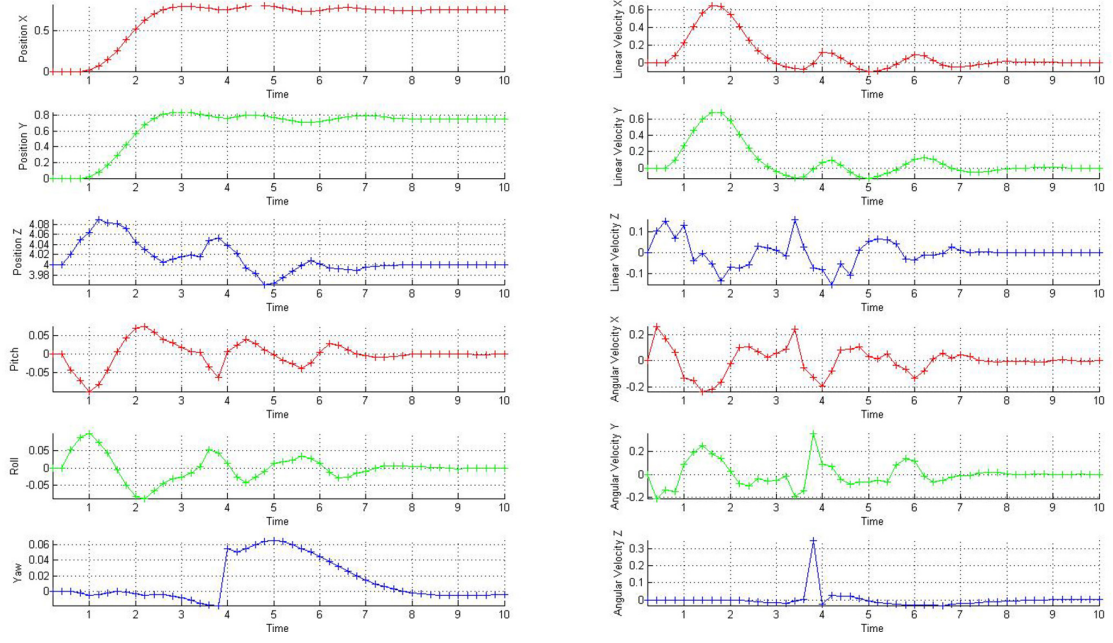


FIGURE 4.15: State variables for a quadrotor in movement and an arm in movement

TABLE 4.8: Summary of the control for a quadrotor in movement and an arm in movement

Parameters	Value
ISE	6.9
Maximum error	1.19
Time to reach to Steady State	3.75s

Chapter 5

Conclusions and Future Work

5.1 Conclusions

This Section is presenting the conclusions obtained after the work done in this Master's Thesis.

This thesis has proposed a NMPC to control a quadrotor affected by a perturbation. Also it has been presented a method to couple the dynamics of the UAV and the robotic arm. Moreover the algorithm designed and implemented is independent from the parameterized models used to modelize the quadrotor and the arm. So in this thesis it has been described a general algorithm able to be applied with any dynamic model. By using the results of the experiments taken, several conclusions for this project can be reached:

- First of all, it was possible to make a model of the quadrotor by taking parameters from different studies. Also, a model of the robotic arm was made. However, some parameters were modified to increase the perturbation.
- At the light of the results, it can be stated that the NMPC is able to control a quadrotor with dynamic perturbations. The behaviour in the five scenarios have been accurate and with a low error. Moreover, has checked the relevance of the horizon control to guarantee to reach to steady state and its impact in the CPU performance.

- All these cases are based in a simulation environment because the code is not optimized enough to test it with real quadrotors. Actually, each simulation takes between 30-40 minutes to obtain all the results.
- In order to minimize the impact of the perturbation, it is important to design smooth motions of the arm.
- After all these simulations it is possible to conclude that the most important parts of the algorithm are the dynamic model of the plant and the control horizon:
 - An accurate model allows to predict the behaviour of the system and then find the optimal control. If the model and the real plant are significantly different the control signals can not bring the system to a desired state.
 - On the other hand, depending of the maneuver, the horizon has to be enough to predict and control the behavior of the system. If the horizon is not large enough, the system has not time to control its inertia and reach to the desired state variables. For a quadrotor in a fixed position, a large horizon is not necessary because the system is near of its desired point. But for quadrotor in movement, in order to reach to a specific position and not surpass it, the horizon has to be enough to let time to control the reactions.

5.2 Future Work

During the steps of this project new interesting topics have appeared to be studied in depth. Some of them are just improvement of the project here presented, and others are new fields of study to expand the control possibilities of the quadrotor.

In this way, a nice research could be optimize the code to implement it to a real system. In order to do it, would be important to reduce the computational time by applying a faster solver of the problem. Also, it would be interesting develop an algorithm able to calculate the minimum control horizon necessary to stabilize the current dynamics of the system. Updating this horizon, the system would always calculate only the necessary steps to control the quadrotor and a lot of operations would be avoided.

Other important task would be to study the effect of change the dynamic of the arm by modifying its parameters online. This effect would simulate when the arm starts to carry some object in its end-effector or if some joints start to fail.

Also it would be interesting to develop a method to change the application point of the arm perturbations to a generic point of the quadrotor. In order to achieve it, it is necessary to study the effects due to apply a force and a torque in a different point of the CoG of the whole system.

Finally, another important research would be include the state variables of the joints and the end-effector inside the NMPC. By this technique would be obtained a more accurate control of the system. Also it would be possible to include a cost function of the end-effector to accomplish some specific tasks.

Bibliography

- Alexis, K., Nikolakopoulos, G., and Tzes, A. (2010). Experimental model predictive attitude tracking control of a quadrotor helicopter subject to wind-gusts. *18th Mediterranean Conf. on Control Automation (MED)*, page 1461–1466.
- Allen, P. K., Timcenko, A., and Yoshimi, B. and Michelman, P. (1993). Automated tracking and grasping of a moving object with a robotic hand-eye system. *Robotics and Automation, IEEE Transactions*, 9:152–165.
- Bangura, M. and Mahony, R. Nonlinear dynamic modeling for high performance control of a quadrotor.
- Bangura, M. and Mahony, R. (2012). Nonlinear dynamic modeling for high performance control of a quadrotor. *Australasian Conference on Robotics and Automation*, pages 1–10.
- Belkheiri, M., Rabhi, A. Hajjaji, A. E., and Pegard, C. (2012). Different linearization control techniques for a quadrotor system. *In 2nd Int. Conf. on Communications, Computing and Control Applications (CCCCA)*, pages 1–6.
- Benallegue, A., Mokhtari, A., and Fridman, L. (2006). Feedback linearization and high order sliding mode observer for a quadrotor uav. *Workshop on Variable Structure Systems*, pages 365–372.
- Bicchi, A. and Tonietti, G. (2004). Fast and” soft-arm” tactics [robot arm design]. *Robotics and Automation Magazine*, 11:22–33.
- Bouabdallah, S. (2007). Design and control of quadrotors with application to autonomous flying. Master’s thesis.

- Bouabdallah, S., Pierpaolo, M., and Siegwart, R. (2004). Design and control of an indoor micro quadrotor. *IEEE International Conference*, 5:4398.
- Bouffard, P. (2012). On-board model predictive control of a quadrotor helicopter: Design, implementation, and experiments. Master's thesis, CALIFORNIA UNIV BERKELEY DEPT OF COMPUTER SCIENCES.
- Bresciani, T. Modelling, identification and control of a quadrotor helicopter. Master's thesis, Lund University Dept Of Automatic Control.
- Corke, P. (2011). *Robotics, vision and control: fundamental algorithms in MATLAB*. Springer.
- Featherstone, R. and Orin, D. (2000). Robot dynamics: Equations and algorithms. In *ICRA*, pages 826–834.
- Fukuda, T. (1985). Flexibility control of elastic robotic arms. *Journal of Robotic Systems (ISSN 0741-2223)*, 2:73–88.
- Grancharova, A., Grotli, E., and Johansen, T. (2012). Distributed mpc-based path planning for uavs under radio communication path loss constraints. Master's thesis.
- Gruene, L. and Pannek, J. (2011). *Nonlinear Model Predictive Control. Theory and Algorithms*. Springer.
- Hayati, S. (1986). Hybrid position/force control of multi-arm cooperating robots. *Robotics and Automation. Proceedings. 1986 IEEE International Conference*, 3:82–89.
- Herrera, R. T., Alcantara, S., Meda, J., and Velazquez, A. (2012). *Kinematic and Dynamic Modelling of Serial Robotic Manipulators Using Dual Number Algebra*.
- Hussein, W. M. Quadrotor design, simulation and implementation. Master's thesis, Arab Academy of Science and Technology.
- Johnson, W. (1994). *Helicopter Theory*. Dover.
- Khosla, P. K. and Kanade, T. (1987). An algorithm to estimate manipulator dynamics parameters.
- Kis, L. and Lantos, B. (2011). Sensor fusion and actuator system of a quadrotor helicopter. *Electrical Engineering*, 53(3-4):139–150.

- Leishman, J. G. (2002). The breguet-richet quad-rotor helicopter of 1907. *Vertiflite*, 47:58–60.
- Martinez, V. (2007). Modeling of flight dynamics of a quadrotor helicopter. Master's thesis, University School of Engineering, Aerospace Sciences.
- Mellinger, D. and V., K. (2011). Minimum snap trajectory generation and control for quadrotors. *Int. Conf. on Robotics and Automation (ICRA)*, pages 2520–2525.
- Nonami, K. (2006). Prospect and recent research and development for civil use autonomous unmanned aircraft as uav and mav. *Journal of system Design and Dynamics*, 1:120–128.
- Noth, A., Bouabdallah, S., and Siegwart, R. (2004). Pid vs lq control techniques applied to an indoor micro quadrotor. *International Conf. on Intelligent Robots and Systems*, pages 2451–2456.
- Oleg, Y. (2009). Development and testing of the miniature aerial delivery system snowflake. *20TH AIAA Aerodynamic deceleration systems technology conference and seminar*.
- Pounds, P. (2007). Design, construction and control of a large quadrotor micro air vehicle. Master's thesis, AUSTRALIAN NATIONAL UNIVERSITY.
- Pounds, P., Mahony, R., and Corke, P. (2006). Modelling and control of a quad-rotor robot. *Proceedings Australasian Conference on Robotics and Automation*.
- Raemaekers, A. (2007). Design of a model predictive controller to control uavs. Master's thesis.
- Romero, H., Salazar, S., and Lozano, R. (2009). Real-time stabilization of an eight-rotor uav using optical flow. *Robotics, IEEE Transactions*, 25:809–817.
- Sanramaria, A. and Andrade, J. (2014). Hierarchical task control for aerial inspection. *euRathlon-ARCAS Workshop and Summer School on Field Robotics*.
- Shin, J., Fujiwara, D., Nonami, K., and K., H. (2005). Model-based optimal attitude and positioning control of small-scale unmanned helicopter. *Robotica*, 23:51–63.
- Sydney, N., Smyth, B., and Paley, D. A. (2013). Dynamic control of autonomous quadrotor flight in an estimated wind field.

- Velliste, M., Perel, S., Spalding, M. C., Whitford, A. S., and Schwartz, A. B. (1995). Cortical control of a prosthetic arm for self-feeding. *Nature*, 453:1098–1101.
- Vries, E. and Subbarao, K. (2010). Backstepping based nested multi-loop control laws for a quadrotor. *Int. Conf. on Control Automation Robotics Vision (ICARCV)*, pages 1911–1916.
- Wai Weng, K. (2006). Design and control of an indoor micro quadrotor. *Research and Development, 2006. SCOReD 2006*, pages 173 – 177.
- Zhu, B. and Huo, W. (2010). Trajectory linearization control for a quadrotor helicopter. *IEEE Int. Conf. on Control and Automation (ICCA)*, pages 34–39.